M+R

E-SF10610

RESEARCH ON LATTICE-MISMATCHED SEMICONDUCTOR LAYERS

DOE/SF/10610--T1

FINAL REPORT

November 1980

Sponsored by:

U. S. DEPARTMENT OF ENERGY
Office of Basic Energy Sciences, OER

Contract No. DE-AC03-79SF10610

Prepared by:

C. Burleigh Cooper III

Varian Associates, Inc.
Solid State Laboratory
Palo Alto, CA 94303

DE81022301

Contract No. DE-AC03-79SF10610

RESEARCH ON LATTICE-MISMATCHED SEMICONDUCTOR LAYERS

Final Report

(September 24, 1979 -- September 24, 1980)

November 1980

Performed by:

Varian Associates, Inc.
Solid State Laboratory
Palo Alto, CA 94303

by

C. Burleigh Cooper III

Sponsored by:

Office of Basic Energy Sciences, OER
Department of Energy
Washington, D.C.

ABSTRACT

The epitaxial growth of AlGaAsSb and the component binary and ternary alloys by organometallic vapor phase epitaxy (OM-VPE) is reported. OM-VPE growth of the binary compounds, GaAs and GaSb, and ternary compounds, AlGaAs, AlGaSb, AlAsSb, and GaAsSb, are discussed with emphasis on the Sb-containing alloys. Growth parameters are reviewed in some detail. It is noted that the growth temperatures and ratio of input fluxes for the growth of Sb-rich alloys are considerably different from the conditions for the growth of As-rich alloys. The results from the study of the binary and ternary components are integrated to grow the quaternary, AlGaAsSb. The work has contributed substantially to the exploration of III-V compound materials which can be grown by OM-VPE.

TABLE OF CONTENTS

* Published Literature & Preprints removed

1. INTRODUCTION

The monolithic multijunction solar cell has been proposed as a way of achieving high photovoltaic conversion efficiency from a single device. The structure consists of low- and high-bandgap cells interconnected by suitable shorted junctions. Several III-V material systems encompass lattice constants and bandgaps suitable for the growth of multijunction cells. At this point, no single quaternary is clearly superior. However, AlGaAsSb is promising for a number of reasons. Figure 1 shows the phase diagram for this quaternary, including bandgaps and lattice constants. Several possible substrate materials are included within the lattice constants spanned by the quaternary. The multijunction device could be entirely grown lattice matched to InP or on a GaAs substrate on which a graded GaAsSb layer had been deposited.

Theoretical aspects of the multijunction concept are well understood, but the reduction to practice requires the solving of many basic materials problems. The work described below is directed toward solving some of the basic materials problems associated with the AlGaAsSb quaternary.

The multijunction solar cell puts stringent requirements on the epitaxial technique used to grow the cell. The technique must be capable of producing a complex multilayer structure containing several different alloy compositions with different doping levels. Organometallic vapor phase epitaxy (OM-VPE) is particularly well suited for the growth of the multijunction monolithic solar cell. Work in our laboratories has shown that OM-VPE is capable of producing epitaxial layers that are uniform in thickness, alloy compositions and doping composition.[1] Different alloys can be readily grown simply by adjusting the input fluxes. In addition, very abrupt junctions can be produced by OM-VPE and the technique is readily automated, which is an important consideration for any large-scale production.

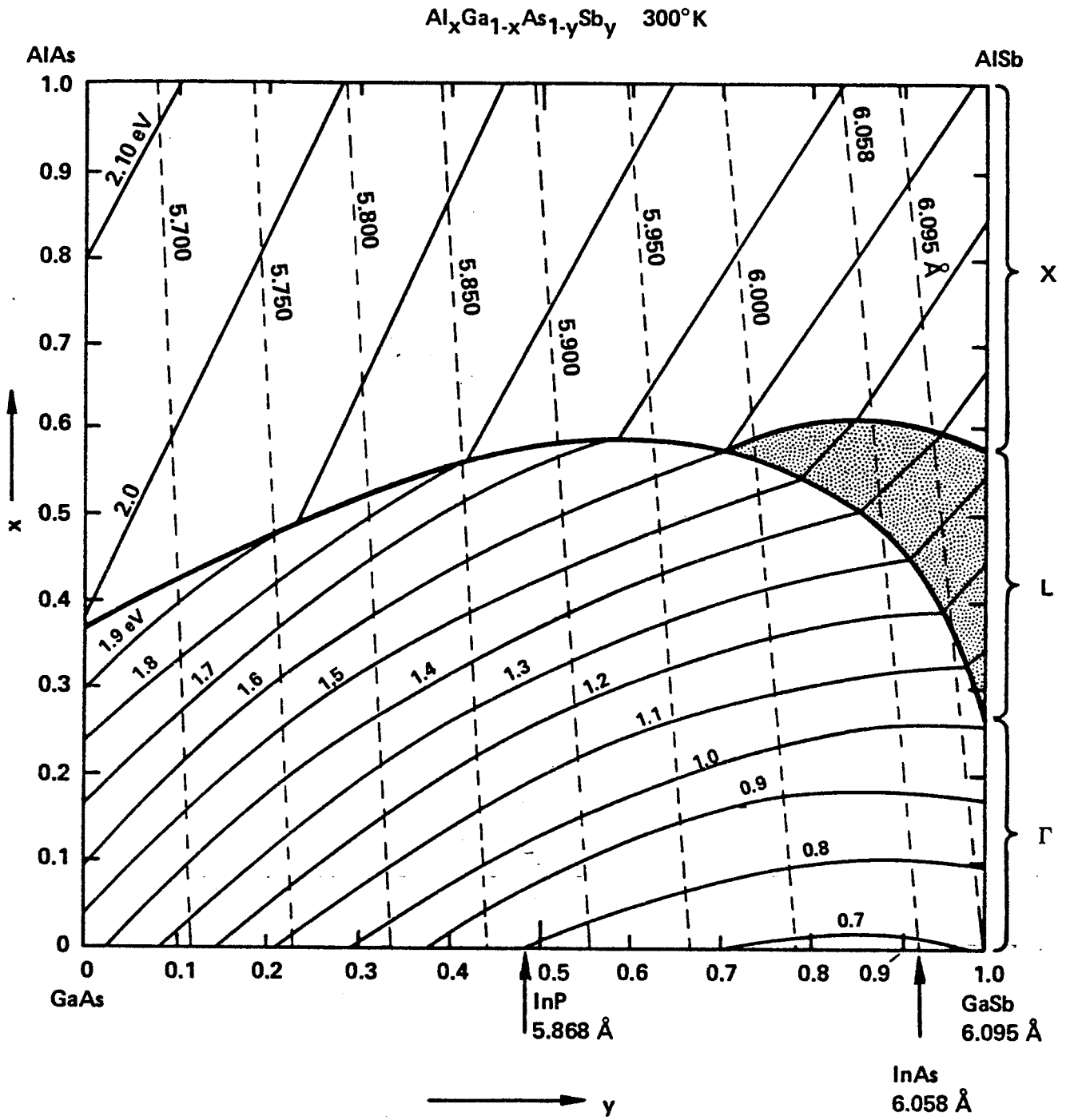

Fig. 1 Phase diagram for AlGaAsSb showing bandgap energies and lattice constants.

2. RESULTS AND DISCUSSION

The prime goal of this research was to learn how to grow the AlGaAsSb quaternary by OM-VPE. The approach adopted consisted of first gathering data on the OM-VPE growth of the component binary and ternary compounds. This data was then integrated to allow growth of the quaternary. The results are briefly summarized in the following sections. Additional information is detailed in the papers concerning this work (Appendix A).

2.1 GaAs

Excellent quality GaAs epitaxial layers have been grown in our laboratories and also have been described by others.[2,3] This important semiconductor can be deposited over a wide range of temperatures and parameters. A typical p-type dopant is Zn, with S and Se serving as typical n-type dopants. The surfaces are generally uniform and free of hillocks or other growth defects.

2.2 AlGaAs

This ternary has received considerable attention from OM-VPE researchers interested in opto-electronic applications.[4,5] Aluminum is readily substituted for gallium by altering the input fluxes of trimethylaluminum (TMAl) and trimethylgallium (TMGa). Figure 2 illustrates this linear relationship graphically. Ready control of alloy composition is an important feature of OM-VPE, as will be discussed in more detail below. The electrical properties of OM-VPE-grown AlGaAs are somewhat disappointing. It is thought that the addition of Al to the crystal results in the gettering of impurities (perhaps oxygen and water) from the OM-VPE system into the crystal. However, recent studies indicate that this problem can probably be circumvented.[6] The surface

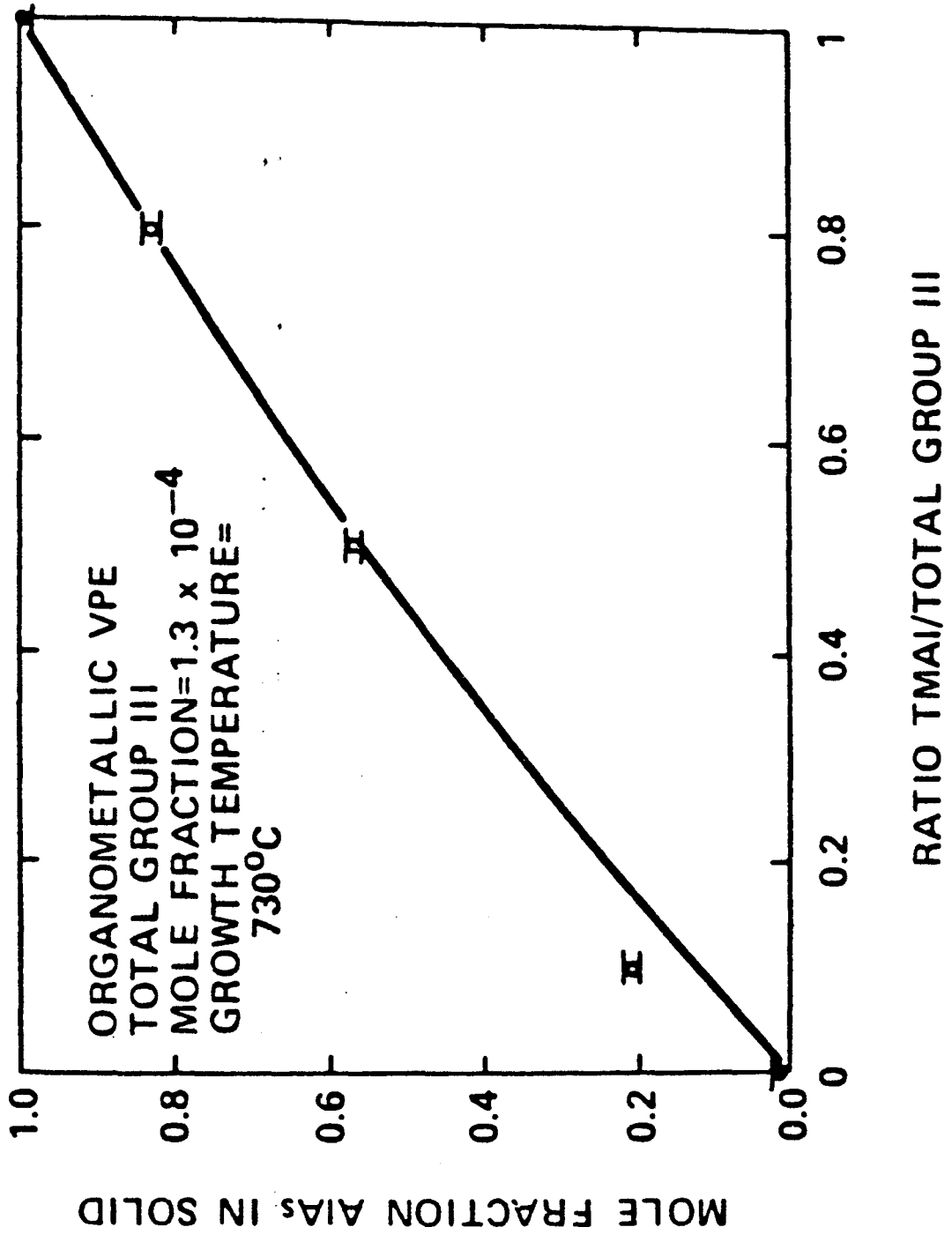

Fig. 2 Percent AlSb versus TMAl to total Group III ratio.

morphologies of AlGaAs layers are excellent over the entire range of the alloy. Zinc and Se serve as suitable p-type and n-type dopants, respectively.

2.3 GaSb

Previous work in our laboratory under Contract EY-76-C-03-1250 indicated that the growth conditions for GaSb are considerably different from the corresponding As-containing alloy. Manasevit recently reported preliminary results on the OM-VPE growth of GaSb, but he did not discuss optimized growth parameters. The chief differences between GaAs and GaSb growth are growth temperature and input flux ratios. Most arsenic-containing semiconductors are grown with a Group V to Group III ratio between 5 and 10. Gallium antimonide epitaxial layers must be grown from a Group III rich vapor (Fig. 3). Superior surface morphology is obtained for growth temperatures in the range 550° to 600°C (Fig. 4).

2.4 GaAsSb

The conditions used for GaSb and GaAs growths were integrated to grow GaAsSb. Epitaxial growth was studied starting from both the As-rich (on GaAs substrates) and Sb-rich (on InAs substrates) sides of the phase diagram (Fig. 1). The surface morphology of the layers is, in general, quite good considering the lattice mismatch between the substrate and final epitaxial composition (Figs. 5 and 6).

The relationship between Sb content in the solid and the trimethyl-antimony (TMSb) to total Group V input ratio is illustrated in Fig. 6. It was not possible to grow epitaxial layers with Sb content between 0.26 and 0.62, as determined by X-ray diffraction. This region may correspond to the miscibility gap which has been discussed for Sb systems.[7,8] It should be noted that growth of GaAsSb layers by molecular beam epitaxy

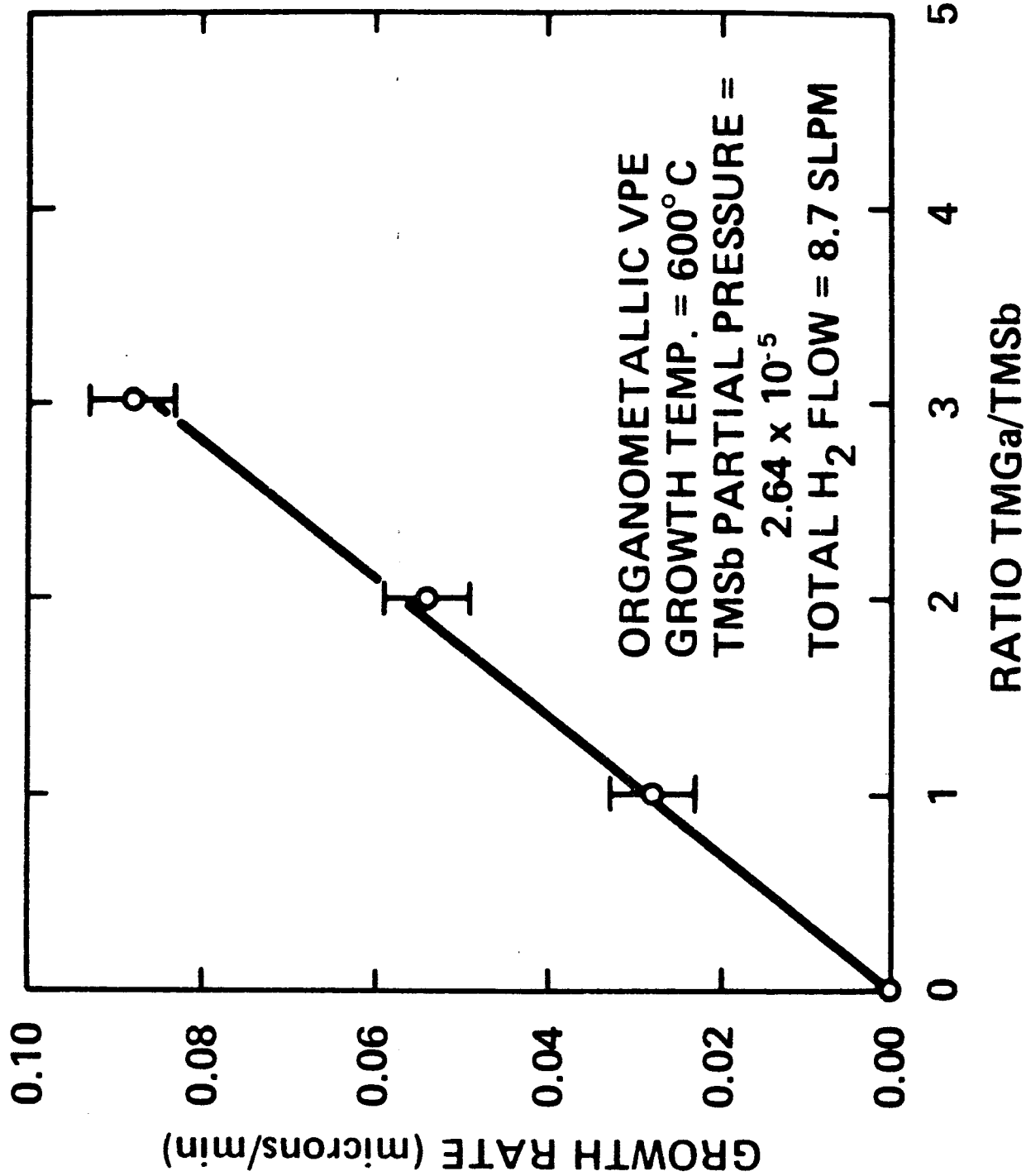

Fig. 3 Relationship between the growth rate and the TMGa-to-TMSb ratio for OM-VPE-grown GaSb.

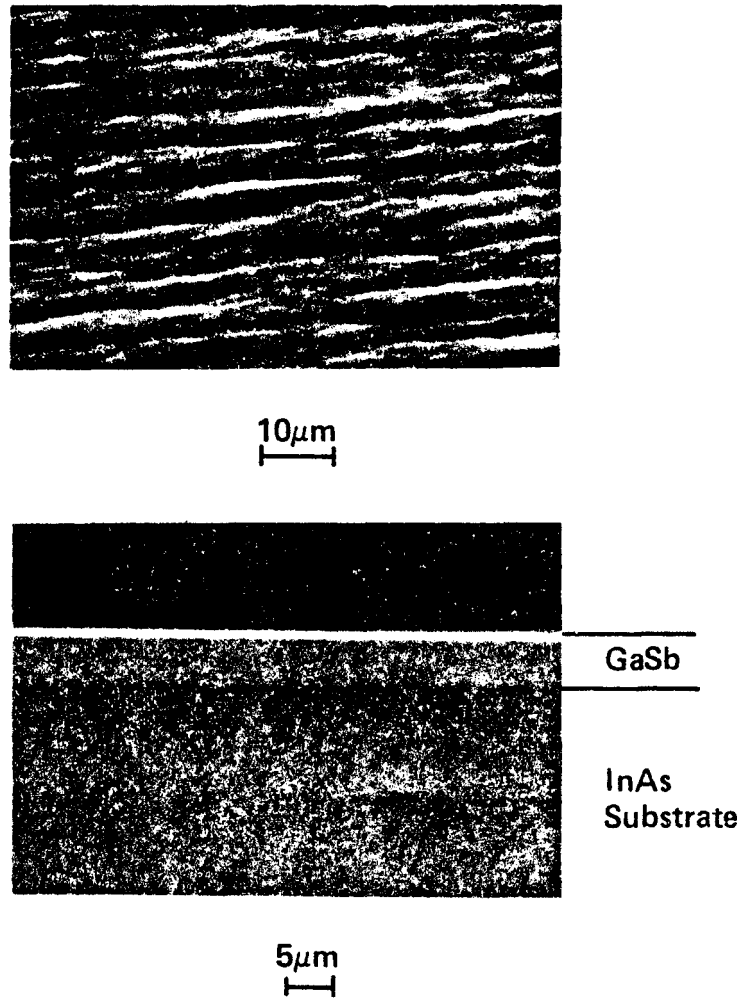

Fig. 4 Surface and cross-section of OM-VPE-grown GaSb epitaxial layer on an InAs substrate.

ORGANOMETALLIC VPE

10μm

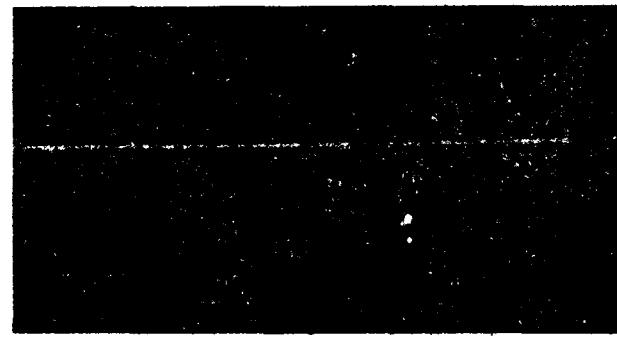

5μm

Fig. 5 Surface and cross-section of OM-VPE-grown $GaAs_{.74}Sb_{.26}$ epitaxial layer on a GaAs substrate.

ORGANOMETALLIC VPE

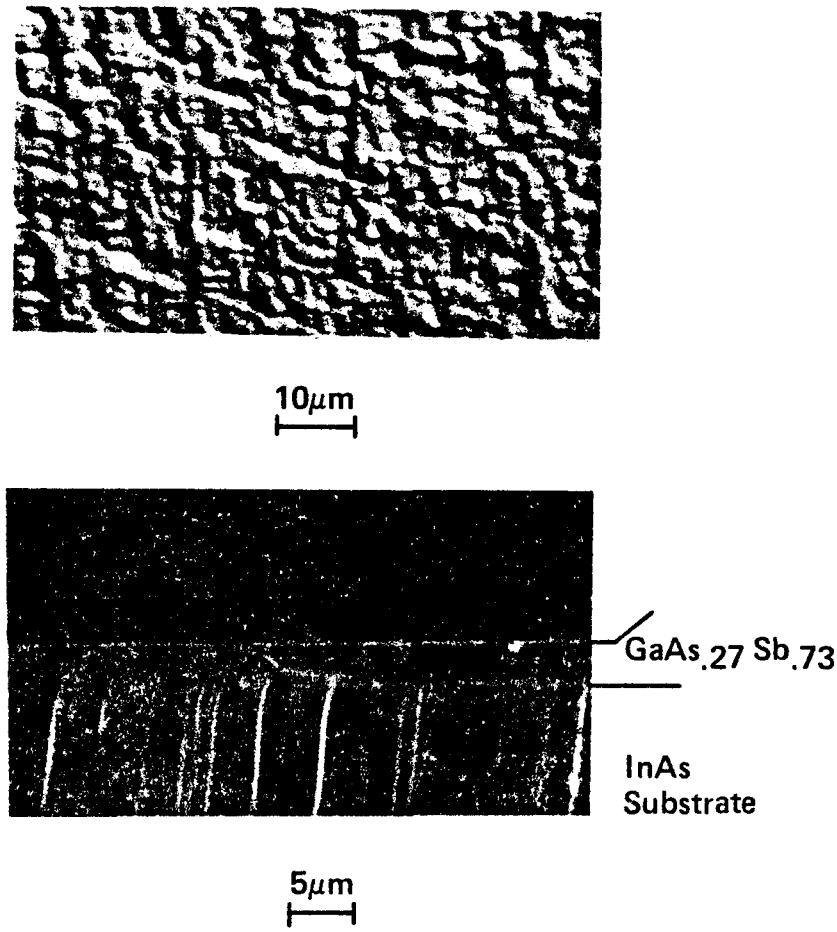

Fig. 6 Surface and cross-section of OM-VPE-grown $GaAs_{.27}Sb_{.73}$ epitaxial layer on an InAs substrate.

within this composition region has been reported.[9] It is possible that the difficulty in growing in this region may be due to lattice-mismatch problems. Both GaAs and InAs substrates are sufficiently different in lattice constant from $GaAs_{.5}Sb_{.5}$ that growth problems might occur. For example, a GaAsSb layer was grown in the OM-VPE reactor which exhibited good surface morphology. It was not possible to determine the composition by X-ray diffraction, but electron-beam microprobe results showed that the Sb content was approximately 0.4. It was possible to start with a GaAs substrate and, through a crude step-grading sequence, to grow several GaAsSb layers of increasing Sb concentration and end growth with a GaSb layer.

Experiments were conducted with InP substrates which have a lattice constant corresponding to $GaAs_{.45}Sb_{.55}$. Growth of a GaAsSb layer lattice matched to a substrate should help solve the miscibility gap problem. This work was commenced near the end of the contract and, owing to the difficulty in stabilizing InP substrates in the organometallic system, it was not possible to grow the lattice-matched GaAsSb layers on InP.

The GaAsSb layers discussed above were grown with AsH_3 as the arsenic source. Experiments were conducted using an alternate As source, trimethylarsine (TMAs). In general, it was noted that the surface morphology and composition were nearly the same regardless of the parent As compound.

2.5 AlAsSb

This ternary compound was investigated in a few experiments. Owing to the high Al content, the wafers were handled in a nitrogen-filled glove box and kept in an inert atmosphere until the analysis was performed. As expected, the growths were similar to the corresponding GaAsSb layers, although growth parameters were not optimized for good surface morphology.

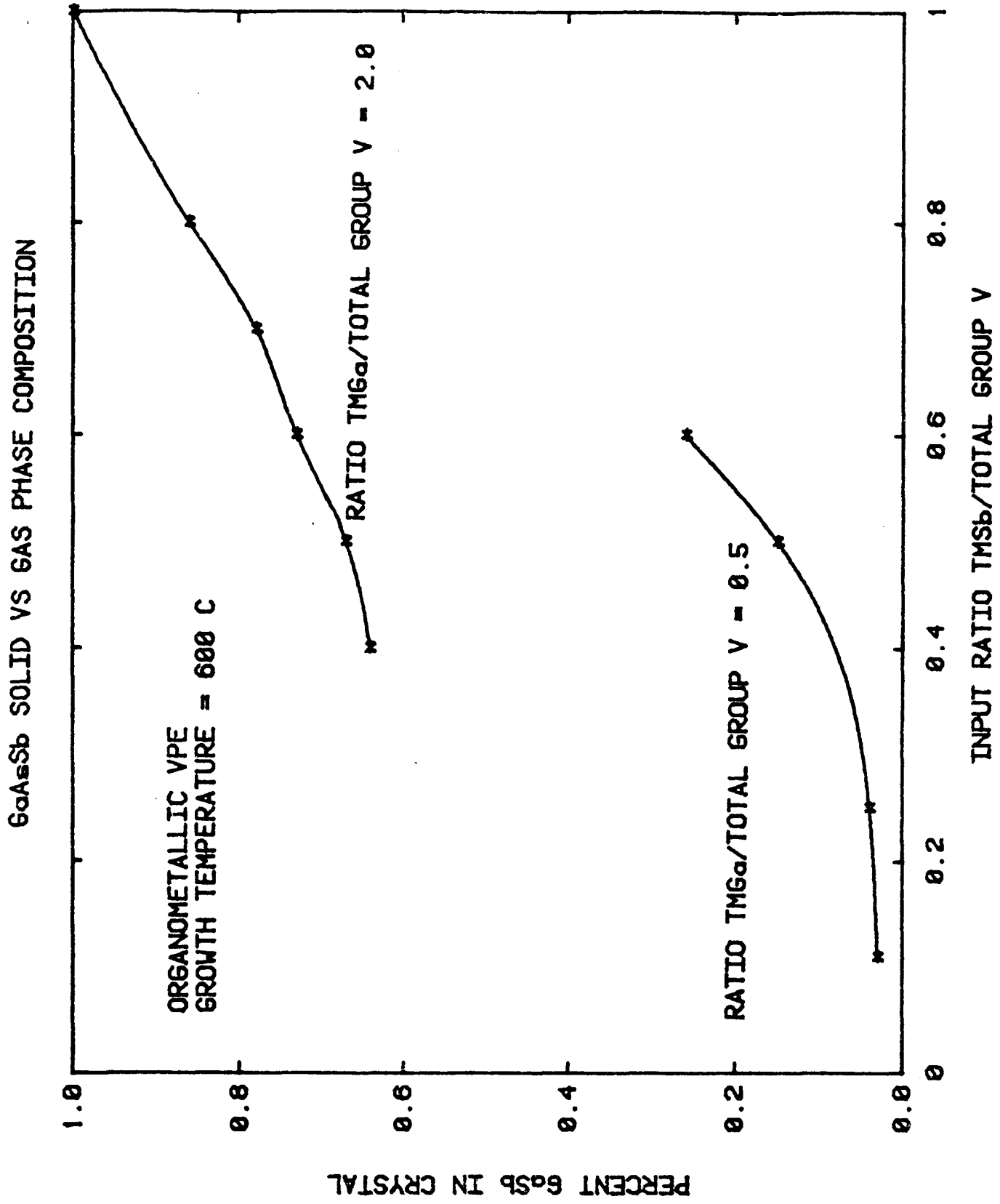

Fig. 7 Relationship between the GaSb content of the solid and the ratio of TMSb to total Group V reactants in the gas phase.

2.6 AlGaSb

The AlGaSb ternary was studied in some detail. All growths were done on InAs substrates; as in the case of other Sb-rich materials, it was necessary to grow from a Group III-rich vapor. Typical surface morphology is illustrated in Fig. 8. The relationship between the AlSb content of the crystal and the ratio of the TMAl to total Group III input flux is illustrated in Fig. 9. The linear relationship was expected, based on the results for AlGaAs discussed earlier.

2.7 AlGaAsSb

A series of experiments was conducted on the quaternary compound. Background data collected on the composite binary and ternary systems proved to be useful. It was possible to predict the growth parameters and composition of the quaternary based on this data. Table I lists the compositions of some representative AlGaAsSb epitaxial layers, as determined by electron-beam microprobe analyses. The surface morphology was, in general, very good as illustrated in Fig. 10.

Figure 11 shows the relationship between the Al content of the crystal and the ratio of the TMAl to total Group III input for the quaternary. As expected, a linear relationship is observed. This is a key feature for the growth of a multijunction solar cell in the AlGaAsSb system. The lattice constant is primarily determined by the As/Sb ratio (Fig. 1), whereas the bandgap is for the most part controlled by the Al/Ga ratio (Fig. 1). This means that once the layer composition has been graded to an appropriate GaAsSb concentration, then the required bandgaps for the high- and low-gap cell can be spanned simply by regulating the TMAl and TMGa input fluxes.

It should be noted that this work resulted in the first reported growth of the AlGaAsSb quaternary by OM-VPE. Furthermore, it represents only the second report of any quaternary grown by OM-VPE.

ORGANOMETALLIC VPE

$Al_{.4}Ga_{.6}Sb$ on InAs Substrate

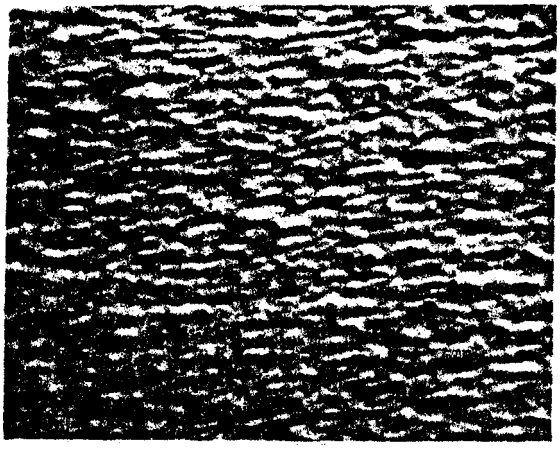

10 μm

Fig. 8 Surface morphology of $Al_{.4}Ga_{.6}Sb$ epitaxial layer on an InAs substrate.

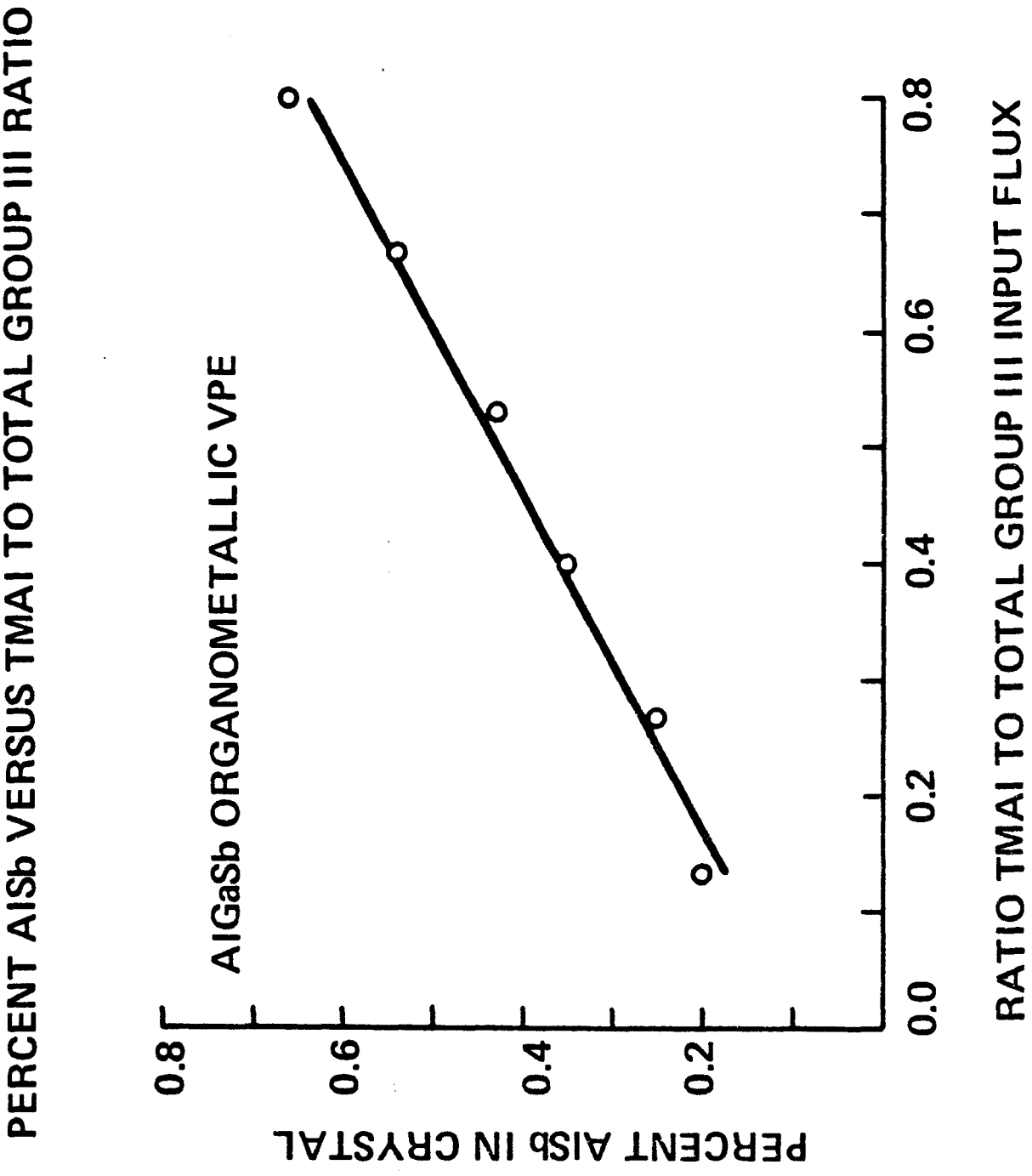

Fig. 9 Relationship between the percent AlSb in the crystal and the ratio of TMAl to total Group III input flux for OM-VPE-grown AlGaSb.

Table I

Electron Microprobe Analysis of AlGaAsSb Epitaxial Layers*

Sample	Al_x	Ga_{1-x}	As_y	Sb_{1-y}
1	.33	.65	.75	.25
2	.40	.61	.77	.23
3	.63	.39	.76	.23
4	.72	.29	.82	.16

*Owing to some uncertainties in the microprobe results, atomic fractions may not add exactly to unity.

ORGANOMETALLIC VPE

$Al_{.3}Ga_{.7}As_{.7}Sb_{.3}$ on GaAs Substrate

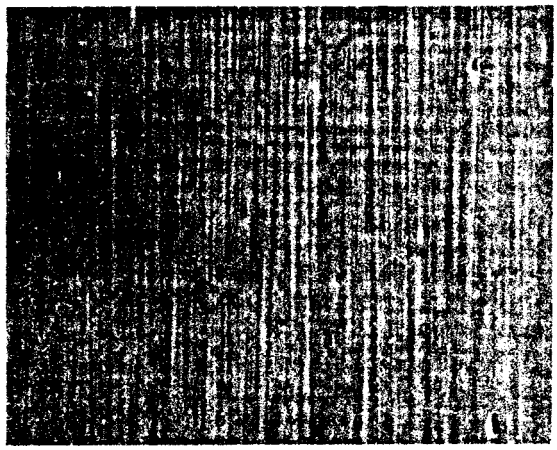

10 μm

Fig. 10 **Surface of $Al_{.3}Ga_{.7}As_{.7}Sb_{.3}$ epitaxial layer on a GaAs substrate.**

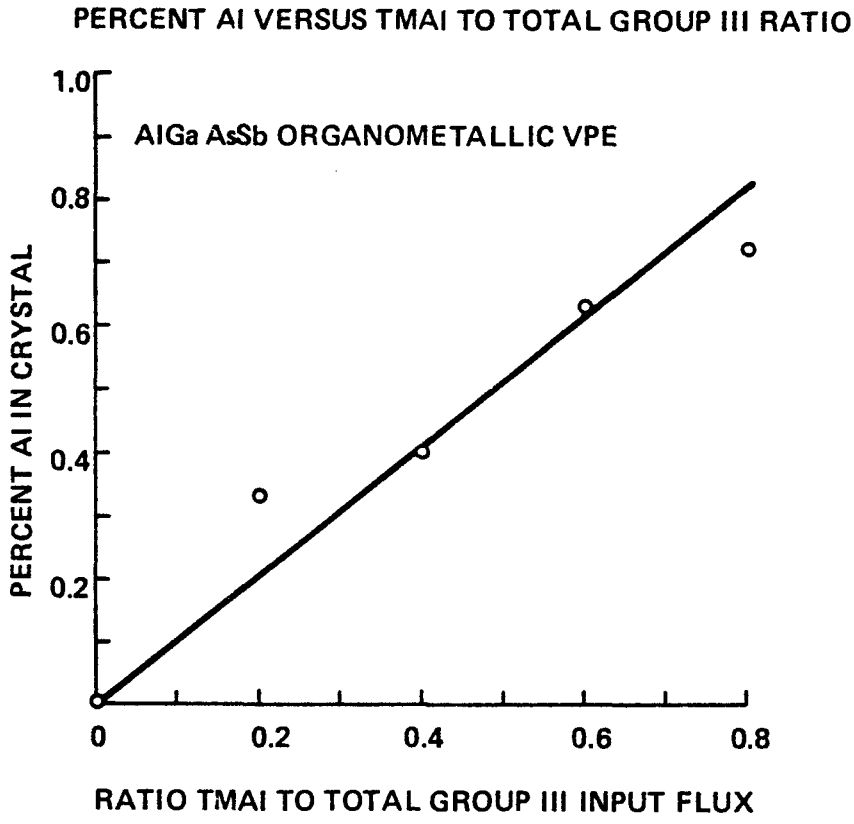

Fig. 11 Relationship between the Al fraction in the solid crystal and the ratio of TMAl to total Group III input flux for OM-VPE grown AlGaAsSb epitaxial layers.

3. SUGGESTIONS FOR FUTURE RESEARCH

This work has contributed substantially to exploration of III-V compound materials which can be grown by OM-VPE. Some aspects of the basic properties of OM-VPE grown AlGaAsSb, however, were not addressed. Background doping of the quaternary should be examined and suitable intentional p- and n-type dopants must be identified. Since the material contains aluminum, some of the problems encountered with AlGaAs (Sec. 2.2) are expected for the quaternary. Research should be conducted which is directed toward evaluating and improving the electrical quality of Al-containing materials.

The most likely substrate for the multijunction solar cell is GaAs, owing to low cost and ready availability. To use this substrate, however, it is necessary to grow a graded GaAsSb layer with a final Sb composition around 0.17 (Fig. 1). Therefore, it would be worthwhile to undertake a study to examine various grading schemes to produce good-quality GaAsSb buffer layers. An evaluation of the grading schemes should include junction performance.

An alternative to the grading discussed above is to grow the entire structure lattice matched to InP substrates. A drawback to this approach is the relatively high cost of the substrates. Some work under this contract was directed toward growths on InP, but a suitable stabilization of the InP substrates in the OM-VPE reactor was not worked out. The InP substrates are lattice matched to a GaAsSb composition in the middle of the so-called miscibility gap. The importance of a demonstration of GaAsSb growth lattice matched to InP is obvious.

Most of the OM-VPE literature reports the results of empirical experiments. Very little is known about the chemistry which occurs in the reactor. Studies to address this area would be extremely valuable

for understanding current processes, for problem solving, and for the design of new systems. The probing of the gas stream by mass spectrometry is probably the best technique to study the chemistry of the OM-VPE reactor.

The final goal of this research is to gain sufficient experience with the AlGaAsSb quaternary (and other OM-VPE materials) to enable the growth of the multijunction monolithic solar cell. Research directed toward this final goal should be pursued.

ACKNOWLEDGEMENTS

The author would like to thank M. J. Ludowise and R. R. Saxena for contributions to this work. Helpful discussions with R. Bell and S. B. Hyder are also acknowledged. Expert technical assistance was provided by N. Anderson, J. Bash, S. Fonte, S. Hikido, L. Mandoli and J. Unruh.

REFERENCES

1. V. Aebi, C. B. Cooper III, R. L. Moon and R. R. Saxena, submitted to the Journal of Crystal Growth.

2. H. M. Manasevit and A. C. Thorsen, J. Electrochem. Soc. 119, 99 (1972).

3. S. J. Bass, J. Crys. Growth 31, 172 (1975).

4. G. B. Stringfellow and H. T. Hall, J. Crys. Growth 43, 47 (1978).

5. G. B. Stringfellow and H. T. Hall, J. Elec. Matl. 8, 201 (1979).

6. G. B. Stringfellow and G. Ham, Appl. Phys. Lett. 34, 794 (1979).

7. R. B. Clough and J. J. Teitjen, Trans. Metal AIME 245, 583 (1969).

8. M. F. Gratton, R. G. Goodchild, L. Y. Juravel and J. C. Wooley, J. Elec. Matl. 8, 25 (1979).

9. T. Waho, S. Ogawa and S. Maruyama, Japan. J. Appl. Phys. 16 (1977).

10. H. M. Manasevit and K. L. Hess, J. Electrochem. Soc. 126, 2031 (1979).

APPENDIX A:

Publications under Contract No. DE-AC03-79SF10610

Presented at the Electronic Materials Conference, Ithaca, NY June 1980
Paper to be submitted to Journal of Electronic Materials.

THE ORGANOMETALLIC VPE GROWTH OF GaSb AND GaAsSb USING TRIMETHYLANTIMONY*

C. B. Cooper III, R. R. Saxena and M. J. Ludowise

Varian Associates, Inc.
Corporate Solid State Laboratory
Palo Alto, CA 94303

ABSTRACT

The organometallic vapor phase epitaxial (OM-VPE) growth of GaSb and $GaAs_{1-x}Sb_x$ ($0 \leq x \leq .26$, $.64 \leq x \leq 1$) is discussed. In both cases, trimethylgallium and trimethylantimony are used as the Ga and Sb source, respectively. Most GaAsSb growths are done using arsine, but the use of an alternate arsenic source, trimethylarsenic, is also reviewed. In contrast to most arsenic-containing alloys, both GaSb and Sb-rich GaAsSb is grown under Group III-rich conditions. The total input flux as well as the ratio of the input chemicals must be closely regulated. In particular, growth of GaAsSb requires careful control of the trimethylantimony-to-total Group V ratio, since arsenic preferentially incorporates into the crystal.

---

*This work was supported by DOE through the Division of Materials Science Branch of the Office of Basic Energy Sciences under Contract No. DE-AC03-79SF10610.

Introduction

Organometallic vapor phase epitaxy (OM-VPE) is becoming an increasingly popular technique for the growth of III-V semiconducting compounds.[1] This interest results from the advantages afforded by OM-VPE as compared to alternate epitaxial techniques. Among these are the growth of a wide range of materials in a single reactor, growth uniformity, both in terms of surface morphology as well as doping and compositional uniformity, the capability of producing multilayer structures and the ease with which the technique can be scaled up and automated. In addition, some alloys which are difficult to grow by other techniques can be readily grown by OM-VPE.[2]

As part of our interest in III-V materials for photovoltaic applications, we have investigated the growth of GaSb and GaAsSb by OM-VPE. Manasevit recently reported preliminary results on the growth of GaSb from trimethylgallium and trimethylantimony.[3] We have studied the growth of GaSb on InAs substrates in detail and report the results below. In addition, we have substantially extended our previous work on the growth of GaAsSb.[4] Data is now available for a wider range of ternary compositions, as well as for the growth of the ternary from all methyl precursors.

Experimental

Epitaxial layers are grown in a horizontal rf induction-heated reactor similar to that described by Bass.[5] Trimethylgallium (TMGa) is used as the Ga source (Alfa) and Group V sources are AsH_3 (10% in H_2, Phoenix Research), trimethylarsenic (TMAs) (Alfa and Strem Chemicals) and trimethylantimony (TMSb) (Alfa). Palladium-diffused H_2 is used as the carrier gas and normally is at a flow rate of 9 slpm. The substrates are single-crystal GaAs (Sn-doped) or single-crystal InAs (Sn-doped), both oriented 2° toward (110) from the (100) plane.

Optimum growth parameters are discussed in detail below. However, most growths of GaSb and GaAsSb are made at a temperature of 600°C with gas phase mole fractions on the order of 10^{-5}.

Both GaAs and InAs substrates are stabilized under an arsine flow until the growth temperature is reached. GaSb growths are made directly on the InAs substrates by stopping the AsH_3 flow when the Ga and Sb sources are introduced. Growth of the ternary compounds are first begun with a thin GaAs (on GaAs substrates) or GaSb (on InAs substrates) layer to initiate nucleation. The appropriate III and V reactants are then introduced into the reactor to grow the ternary of interest.

Analysis of the epitaxial techniques is by several methods. Optical microscopy is used to examine surface morphology and cleaved

cross sections of the wafers. Photoluminescence spectra are recorded for some of the layers. X-ray diffraction is used to verify the single-crystal nature of the GaSb layers. Composition of the GaAsSb growths is checked by electron beam microprobe analyses and by X-ray diffraction.

Results and Discussion

GaSb

The binary compounds GaAs and GaSb are examined as a reference point for the GaAsSb work. The growth of GaAs by OM-VPE is well characterized in our laboratories and the laboratories of others.[5,6] Gallium antimonide, however, is less well characterized. Manasevit recently reported some preliminary results of GaSb growth on a variety of substrates, but he did not discuss optimized growth parameters.[3] This and earlier work demonstrated that the growth conditions are considerably different from those for GaAs.[4] We detail here our results of OM-VPE growth of GaSb epitaxial layers on InAs substrates.

Figure 1 shows a plot of the growth rate versus the TMGa-to-TMSb input ratio. Good quality single-crystal layers are grown from a slightly Group III rich gas phase (TMGa-to-TMSb ratio between 1 and 3). This is in contrast with most arsenic-containing alloys which are grown from Group V rich gas streams.[2] Since both elemental Ga and Sb have

negligible vapor pressures[7] at the growth temperatures, any elements which are deposited on the wafer must be incorporated into the layer if crystal quality is to be maintained. This is readily evident in the growths. Droplets and needles are noted on the wafers if the gas phase ratios are not carefully controlled. In addition, surface morphology deteriorates if the total input of the reactants is too high. The OM-VPE growth of single-crystalline GaSb on InAs takes place in a much narrower range of conditions than some other III-V alloys.[8]

Figure 2 shows the relationship between the growth rate and substrate temperature for GaSb growths from a gas phase consisting of a 2:1 TMGa-to-TMSb ratio. Reasonable surface morphology is noted for substrate temperatures between 550 and 600°C, but the optimum temperature is at the high end of this range. Figure 3 shows a surface and cross section of GaSb on an InAs substrate. The layer was grown at 600°C from a gas phase containing TMGa and TMSb partial pressures of 2.6×10^{-5} and 1.3×10^{-5}, respectively. Under these conditions, the growth rate is on the order of 0.036 μm/min.

GaAsSb

The parameters determined for GaSb and GaAs growths are utilized as a basis for GaAsSb growths. The ternary was first grown from TMGa, AsH_3 and TMSb, and subsequently TMAs was substituted for the As source.

Epitaxial growth is studied starting from both the As-rich (on GaAs substrates) and Sb-rich (InAs substrates) sides of the phase diagram.

Figure 4 shows a plot of GaSb content of the crystal versus the TMSb-to-total Group V ratio for layers deposited on GaAs substrates. Growths are started with a thin GaAs layer to nucleate growth, followed by a crude step grading of thin layers to the final constant composition GaAsSb layer. Typical grading steps for a $GaAs_{1-x}Sb_x$ (x = .26) epitaxial layer include layers with x = 0, 0.04, and 0.15. Total epitaxial thickness was typically on the order of a few microns. The best surface morphology is obtained with TMGa/[total Group V] = 0.5. Typical partial pressures in the gas stream are 1.3×10^{-5} and 2.6×10^{-5} for TMGa and total Group V, respectively. As illustrated in Fig. 4, As is preferentially incorporated over Sb. Under the conditions used in these experiments, the maximum Sb content verified by X-ray diffraction was 26%. Microprobe data on an additional layer of good surface morphology indicates that the epitaxial layer contains 40% Sb. Typical growth rates are on the order of 0.03 to 0.04 μ/min. Photoluminescence spectra were recorded for several of the wafers. The composition calculated[9] from this data generally shows a higher Sb content than that indicated by the X-ray diffraction data. Figure 5 illustrates the surface and cross section of a $GaAs_{.74}Sb_{.26}$ layer deposited on a GaAs substrate. The cross-hatch pattern typical of lattice-matched layers is clearly evident.[10] Hall data on a $GaAs_{.74}Sb_{.26}$ layer deposited on Cr-doped GaAs substrate indicated a background doping on the order of $3.7 \times 10^{16} cm^{-3}$ p-type with an associated 300°K mobility of 1500 cm^2/V-sec.

A similar set of experiments was also conducted starting from the GaSb-rich end of the phase diagram. Growths are started with the deposition of a thin GaSb layer on the InAs substrate. This is followed by a crude step grading to the final composition. Typical steps for $GaAs_{1-x}Sb_x$ (x = .46) are x = 1.0, 0.86, 0.78, 0.73, and 0.67 with a TMGa-to-total Group V ratio of 2.0. Figure 6 shows the results of these experiments. Again, it was possible to grow layers spanning only a limited composition range. The highest As content verified by X-ray diffraction was for a layer with the composition $GaAs_{.36}Sb_{.64}$. As with the layers grown from the GaAs-rich side of the phase diagram, growth rates are on the order of 0.04 μm.

It is possible to start with a GaAs substrate and, through a crude step-grading sequence, to grow several layers of GaAsSb with increasing Sb concentration and end growth with a GaSb layer. The experiment was also performed starting with a GaSb substrate and ending up with a GaAs layer.

In addition to the growths described using AsH_3 as the As source, a series of growths were made with TMAs as the As source. In general, it was noted that the surface morphology and composition were very similar, regardless of whether arsine or TMAs was used.

Conclusions

There has been discussion in the literature regarding the existance of a miscibility gap in the GaAsSb system.[11,12] As described above, it was not possible to grow epitaxial layers with Sb content between 0.26 and 0.64, as verified by X-ray diffraction. Similar results have been noted for GaAsSb growths by halogen VPE.[13] However, there is a report of the growth of GaAsSb epitaxial layers within the so-called miscibility gap by molecular beam epitaxy.[14] In the case of OM-VPE, it is not clear whether factors might be responsible for the lack of X-ray-verified $GaAs_{1-x}Sb_x$ ($.26 \leq x \leq .64$) layers. The lattice mismatch that occurs between GaAs or InAs substrates and $GaAs_{1-x}Sb_x$ ($.26 \leq x \leq .64$) layers may result in deterioration of epitaxial quality.[15] Support for this position is provided by the good-quality $GaAs_{.6}Sb_{.4}$ layer (by electron beam microprobe) which could not be verified by X-ray diffraction. Additional experiments are in progress to determine if single-crystal GaAsSb layers can be grown across the entire composition range by OM-VPE.

Acknowledgement

The authors gratefully acknowledge R. L. Bell for his encouragement and continued support, and helpful discussion with S. B. Hyder. Thanks are also due to N. Anderson, J. Bash, S. Fonte, S. Hikido, L. Mandoli, C. Molinari and J. Unruh for expert technical assistance.

References

1. See, for example, abstracts for Electronic Materials Conference, Ithaca, NY (June 24-27, 1980).
2. G. B. Stringfellow and H. T. Hall, Jr., J. Elect. Matl. 8, 201 (1979).
3. H. M. Manasevit and K. L. Hess, J. Electrochem. Soc. 126, 2031 (1979).
4. C. B. Cooper III, M. J. Ludowise, V. Aebi and R. L. Moon, J. Elect. Matl. 9, 299 (1980).
5. S. J. Bass, J. Crys. Growth 31, 172 (1975).
6. V. Aebi, C. B. Cooper III, R. L. Moon and R. R. Saxena, submitted to J. Crys. Growth.
7. R. E. Honig and D. A. Kramer, RCA Rev. 30, 285 (1969).
8. P. K. Bhattacharya, J. W. Ku, S. J. T. Owen, V. Aebi, C. B. Cooper III and R. L. Moon, Appl. Phys. Lett. 36, 304 (1980).
9. R. E. Nahory, M. A. Pollack, J. C. DeWinter and K. M. Williams, J. Appl. Phys. 48, 1607 (1977).
10. G. H. Olsen and M. Ettenbery in Crystal Growth Theory and Techniques, C. H. L. Goodman (ed.) (Plenum Press, New York, 1978).
11. M. F. Gratton and J. C. Woolley, J. Elect. Matl. 2, 455 (1973).
12. M. F. Gratton and J. C. Woolley, J. Electrochem. Soc. 127, 55 (1980).
13. R. B. Clough and J. J. Tietjen, Trans. Metal. Soc. AIME 245, 583 (1969).
14. T. Waho, S. Ogawa and S. Maruyama, Japan. J. Appl. Phys. 16, 1875 (1977).
15. G. H. Olsen and M. Ettenberg, in Crystal Growth, Vol. 2, ed. C. H. L. Goodman (1978).

Figure Captions

Fig. 1 Relationship between the growth rate and the TMGa/TMSb ratio for OM-VPE-grown GaSb.

Fig. 2 Graph showing the relationship between growth rate and substrate temperature for OM-VPE-grown GaSb.

Fig. 3 Surface and cross-section of GaSb epitaxial layer on InAs substrate.

Fig. 4 Precent GaSb in the solid as a function of the TMSb-to-total Group V input for OM-VPE-grown GaAsSb on GaAs substrates.

Fig. 5 Surface and cross-section of OM-VPE-grown $GaAs_{.74}Sb_{.26}$ on GaAs substrate.

Fig. 6 Percent GaSb in the solid as a function of the TMSb-to-total Group V input for OM-VPE-grown GaAsSb on InAs substrates.

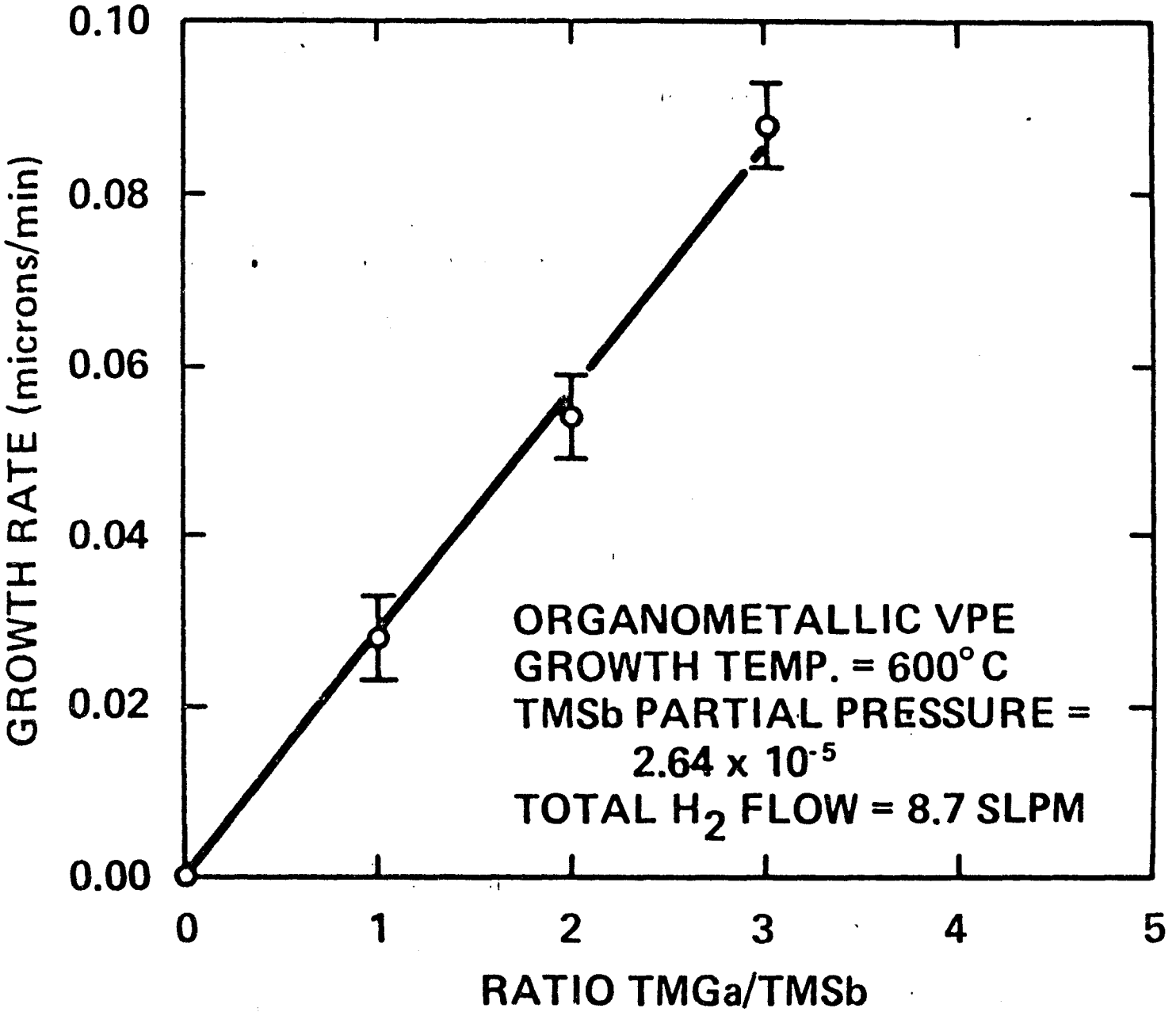
0.10
0.08
0.06
0.04
0.02
0.00
GROWTH RATE (microns/min)
0
1
2
3
4
5
RATIO TMGa/TMSb
ORGANOMETALLIC VPE
GROWTH TEMP. = 600°C
TMSb PARTIAL PRESSURE =
2.64 x 10-5
TOTAL H2 FLOW = 8.7 SLPM

Fig 1

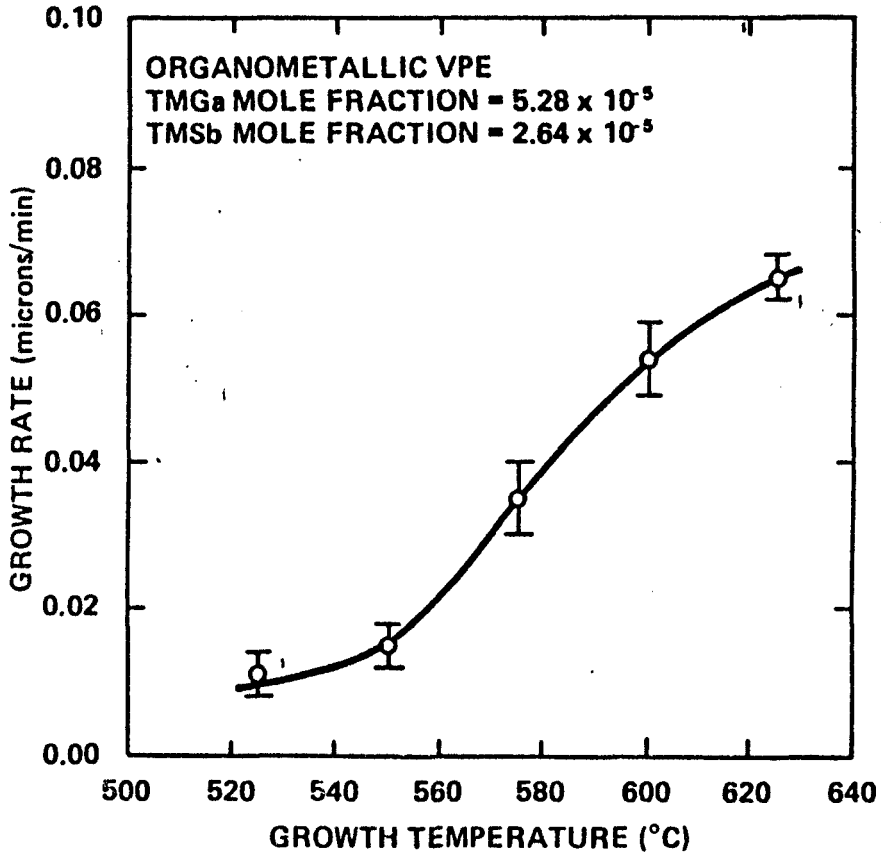
ORGANOMETALLIC VPE
TMGa MOLE FRACTION = 5.28 x 10⁻⁵
TMSb MOLE FRACTION = 2.64 x 10⁻⁵
GROWTH RATE (microns/min)
0.10
0.08
0.06
0.04
0.02
0.00
500
520
540
560
580
600
620
640
GROWTH TEMPERATURE (°C)

GaSb ORGANOMETALLIC VPE

10μm

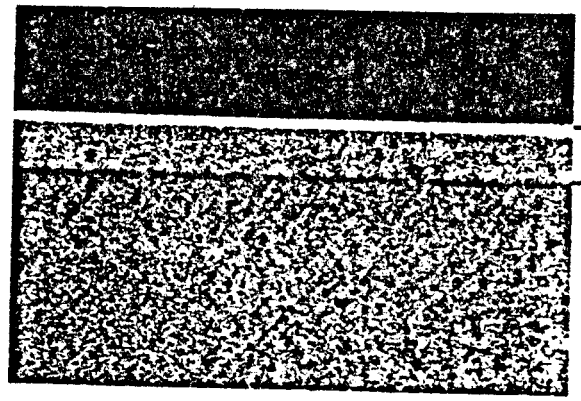

5μm

Fig 3.

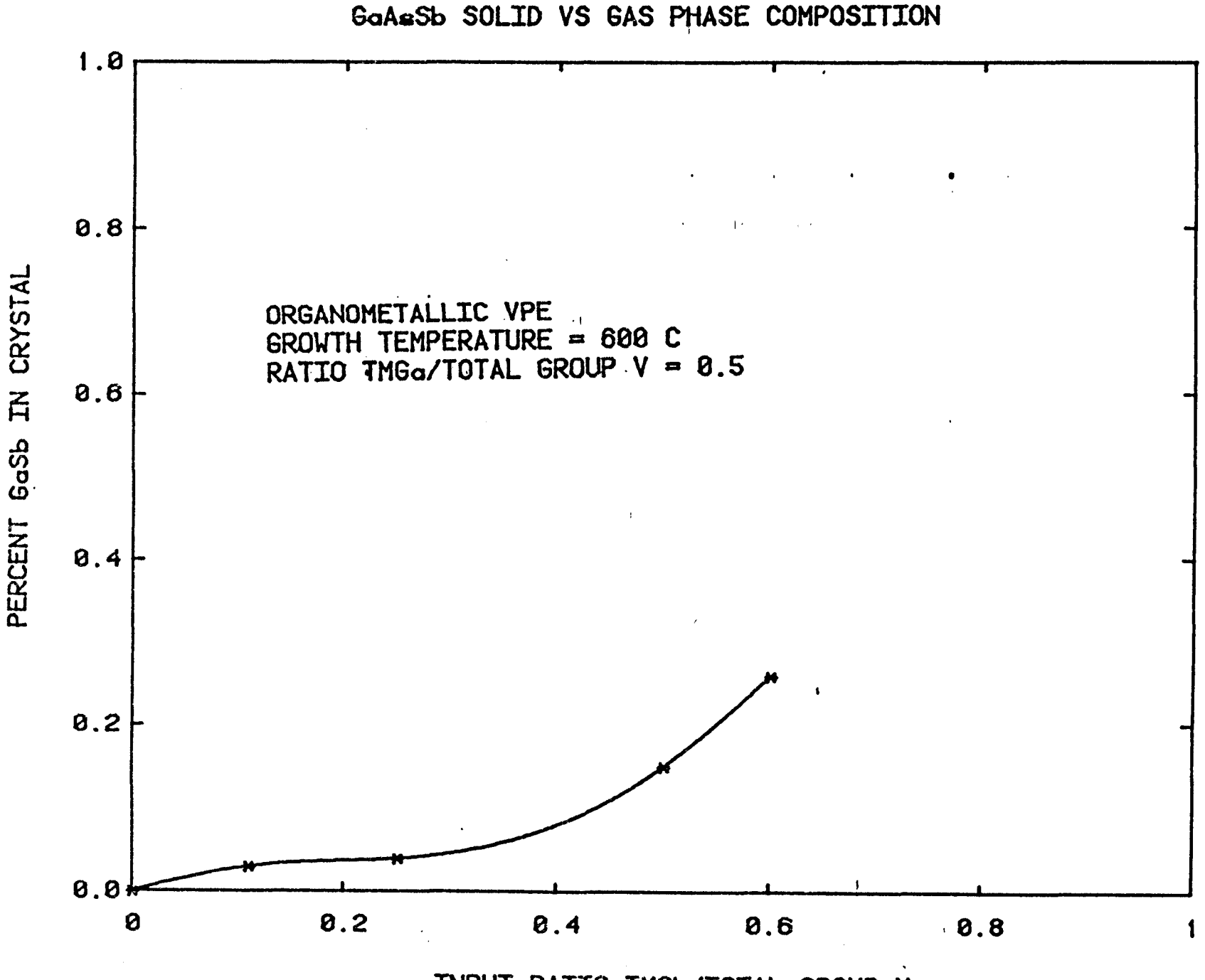
GaAsSb SOLID VS GAS PHASE COMPOSITION
ORGANOMETALLIC VPE
GROWTH TEMPERATURE = 600 C
RATIO TMGa/TOTAL GROUP V = 0.5
PERCENT GaSb IN CRYSTAL
INPUT RATIO TMSb/TOTAL GROUP V
1.0
0.8
0.6
0.4
0.2
0.0
0
0.2
0.4
0.6
0.8
1

Fig 4

ORGANOMETALLIC VPE

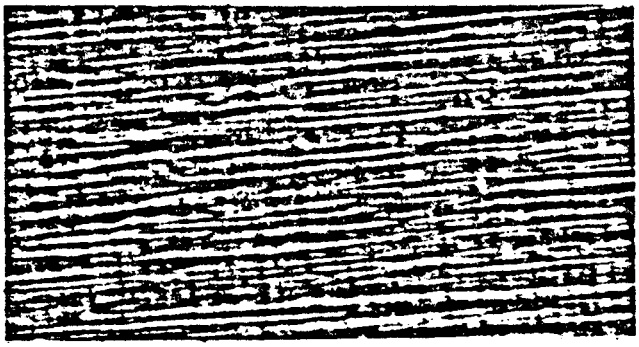

10μm

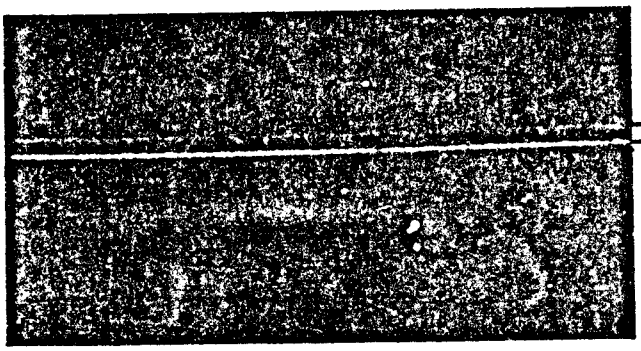

5μm

Fig 5.

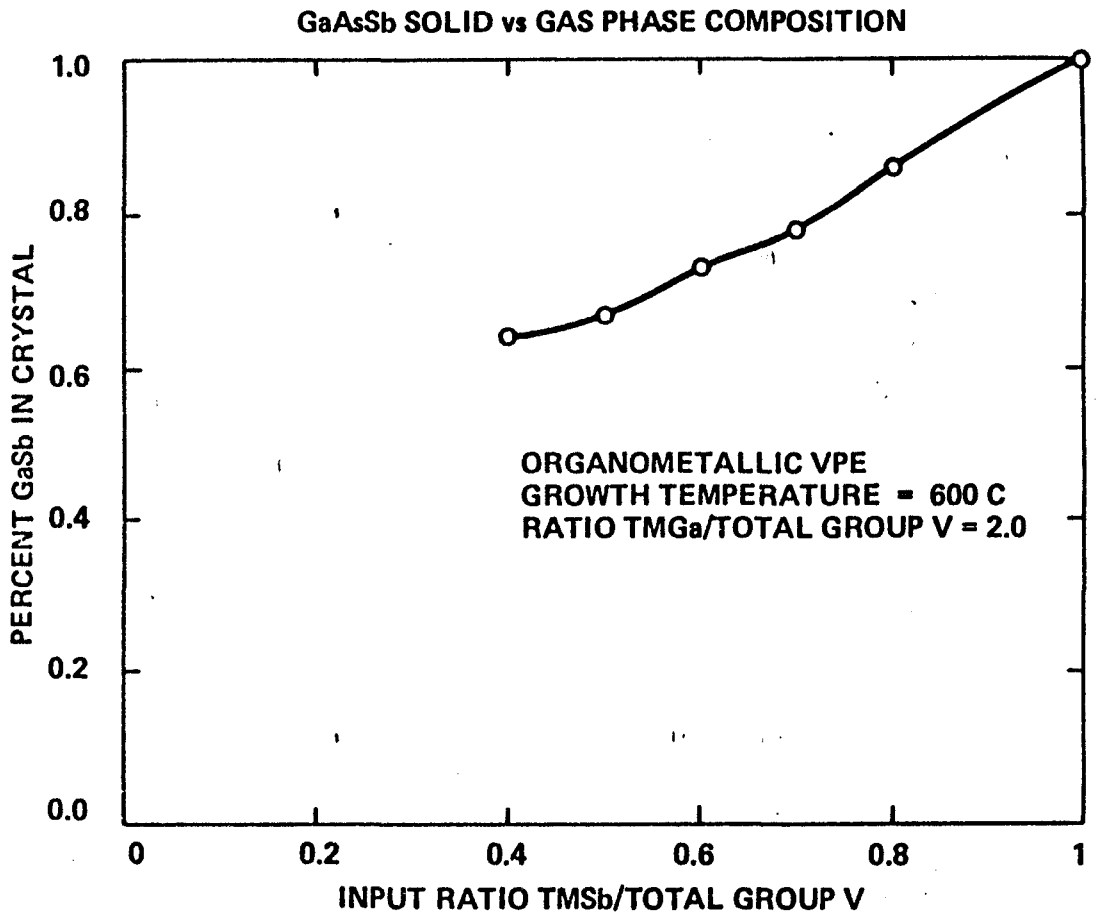
GaAsSb SOLID vs GAS PHASE COMPOSITION
PERCENT GaSb IN CRYSTAL
1.0
0.8
0.6
0.4
0.2
0.0
0
0.2
0.4
0.6
0.8
1
INPUT RATIO TMSb/TOTAL GROUP V
ORGANOMETALLIC VPE
GROWTH TEMPERATURE = 600 C
RATIO TMGa/TOTAL GROUP V = 2.0

APPENDIX B:

Publications under Contract No. EY-76-C-03-1250

Paper presented at the 13th IEEE Photovoltaic Specialists Conference, Washington, D.C., June 1978.

MULTIGAP SOLAR CELL REQUIREMENTS AND THE PERFORMANCE OF AlGaAs AND Si CELLS IN CONCENTRATED SUNLIGHT

R. L. Moon, L. W. James, H. A. Vander Plas,
T. O. Yep, G. A. Antypas and Y. Chai

Varian Associates, Inc.
Palo Alto, CA 94303

ABSTRACT

Multigap solar cells are capable of operating in concentrated sunlight with efficiencies >30%. If only two bandgaps are considered, their optimum values are 1.1 eV and 1.65 eV. Within this energy range Si and Al-Ga-column V alloys are possible materials and their relative merits are discussed. Experimentally, $Al_xGa_{1-x}As$ for X <0.24 and Si have been tested individually and in combination with a spectral splitting filter. In combination a total efficiency of 28.5% including the filter has been observed at 165 AM 1.23 suns. For an ideal filter this corresponds to 31% combined cell efficiency.

INTRODUCTION

The idea of increasing photovoltaic conversion efficiency by using cells with different bandgaps was first proposed by Jackson in 1958 (1). At that time only 1 sun illumination was considered and the attendant complexity could not be economically justified. Since Si and other solar cells had not achieved their projected performance, development of the multigap concept was not pursued.

However, the advent of demonstrably higher power per cell with high efficiencies by the use of concentrated sunlight has refocused attention on the multigap concept (2,3,4,5,6,7). With concentrators the importance of the cost per cell diminishes relative to total systems costs. In turn this allows greater cell design complexity. Absolutely paramount to concentrator system success is the attainment of high efficiencies. A recent EPRI report which deals with photovoltaics applications for utilities exemplifies this point by noting that the viability of high concentration systems requires conversion efficiencies of 25-30% (8).

Attainment of such efficiencies at high concentration appears to be possible only when more than a single junction device is used. Although efficiencies greater than 25% can be obtained for moderate concentrations, realistic modeling that includes most of the pertinent cell parameters and that has been experimentally confirmed, places the maximum efficiency on AlGaAs/GaAs solar cells at 24% for 1000 suns at AM2 (9). The two major energy loss mechanisms and their amount are determined by a single parameter: the solar cell bandgap; photons with energies below bandgap are transmitted and simply lost while those with higher energies are absorbed, but dissipate any excess energy above bandgap in the form of heat (10). Splitting the solar spectrum by using two or more cells (whose bandgaps have been optimally chosen) reduces each form of loss and increases the total efficiency.

Two other loss mechanisms, contact obscuration and series resistance, may be reduced by a multigap arrangement. Since at a given solar flux, the current in each cell is reduced from that of a single cell. Consequently, front contact grids can be redesigned with less obscuration without increased series resistance. Alternatively, the same current could be maintained with a larger optical module, so solar array interconnections and assembly costs could be reduced.

This paper examines some important factors and materials requirements for the operation of a multigap solar cell and describes the successful operation of such an arrangement.

MULTI-GAP CELL REQUIREMENTS

Efficiency of any combination of cells depends upon the choice of bandgaps because losses at some point will be minimized owing to a fixed solar spectrum. A first approximation for determining efficiency as a function of bandgaps is achieved by assuming matching short circuit current in each cell rather than maximum-power load currents (5). For high concentration this approximation involves negligible error

at moderate temperatures since the fill factor and thus the efficiency is determined largely by series resistance effects.

Calculation of efficiencies proceeds then by determining for each lower bandgap the higher bandgap where equality of short circuit current occurs. Spectral response of each cell is idealized by a uniform quantum efficiency (which can be set) between photon energies set by the bandgaps. The efficiency of each cell is calculated by dividing the incident power into the maximum attainable power calculated from the following equations:

$$I_m = I_{sc} = C \cdot I_{sc}(1 \text{ sun})$$

$$V_m = E_g + \frac{kT}{q}\,(\ln C \cdot I_{sc} - 19.1)$$

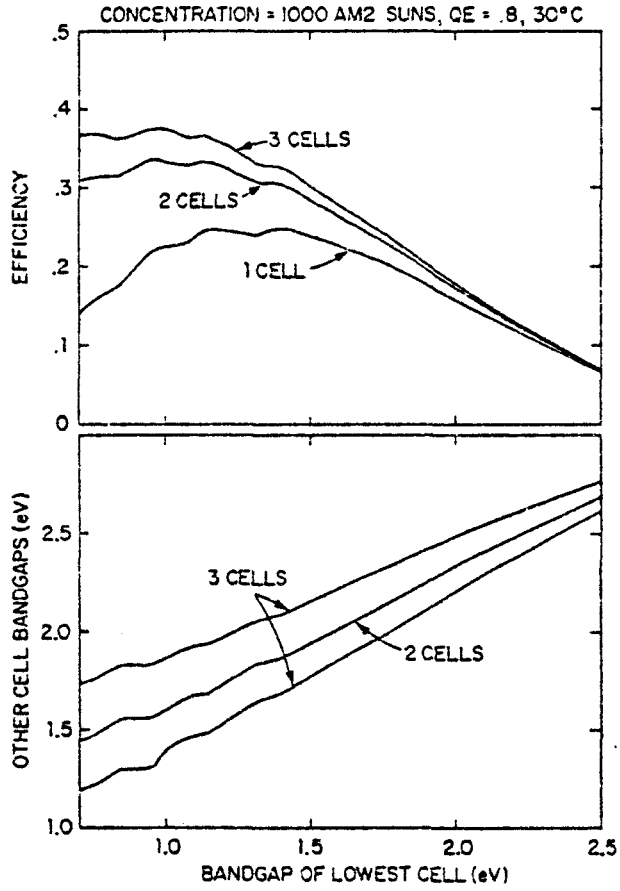

Fig. 1 Potential performance at 30°C of 1,2,& 3 solar cells with 80% quantum efficiency and an illuminating flux of 1000 AM2 suns. Upper curves: efficiency vs bandgap of lowest cell. Lower curves: other bandgaps vs bandgap of lowest cell.

where I_m = current at maximum power, I_{sc} = short circuit current, E_g = bandgap, C = concentration and kT/q has its usual meaning. The expression for V_m follows from the usual expressions for V_{oc} and V_m plus assuming that the reverse saturation current I_o obeys the relationship, $I_o = K\, e^{Eg/kT}$ (6).

Using this approximation, efficiency and distribution of bandgaps are computed for a single, double and triple cell arrangement as a function of the lowest cell bandgap. The results are shown in Fig. 1 for a solar illumination flux of 1000 AM2 suns onto cells with quantum efficiency of 80% held at 30°C. Maximum efficiencies increase from 24.5% to 33.% to 37.5% for 1, 2, and 3 junction cells, respectively. Under these conditions a two bandgap cell could operate within one percentage point of the maximum with lower bandgaps between 0.95 to 1.12 eV and corresponding upper bandgaps of 1.58 to 1.68 eV. For a three bandgap cell operating within 1.5 percentage points of optimum, bandgap ranges are 0.7 to 1.12 eV, 1.2 to 1.48 eV, and 1.75 to 1.93 eV, for the lower, intermediate and upper junctions, respectively. In summary, it is clear that there is some latitude in picking optimum cell combinations and that ultimately the choice is dictated by materials considerations.

The assumption that short circuit current equality produces maximum efficiency has been tested for the two junction case by computing the efficiency variation with varying upper bandgaps, given the lower band, for cells run independently. Fig. 2 shows the results for concentrations of 1 sun and 1000 suns. It can be seen that the optimum efficiency for the pair occurs close to the equal-current condition. Thus, negligible sacrifice in efficiency is made by designing for series operation of the cells.

An important question for multigap cell operation is whether there are diurnal variations of one portion of the solar spectrum relative to another. As a first attempt to answer this question the ratio of short circuit currents from a GaAs solar cell (E_g = 1.425 eV) and an InGaAsP photodiode (E_g = 1.1 eV) have been recorded throughout a day and the results shown in Fig. 3. An overall trend of constancy is seen except for the rapid changes caused by clouds altering the spectrum and the hour or so just before sunset. Solar spectrum variation during the day appears minor from this data, but this is quite preliminary

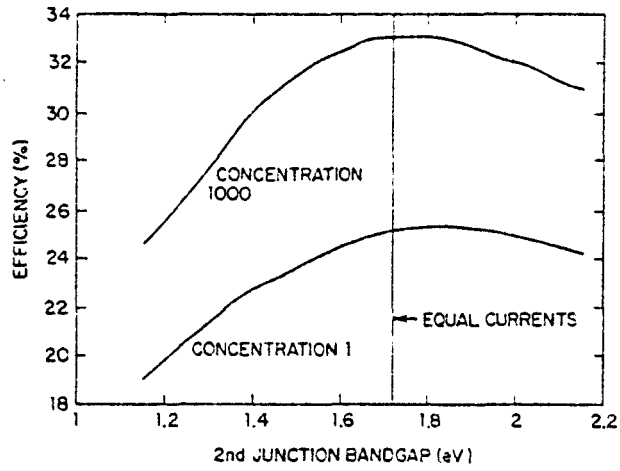

Fig. 2 Two-bandgap conversion efficiency as a function of the upper bandgap, for a lower bandgap of 1.15, and concentration ratios of 1 & 1000.

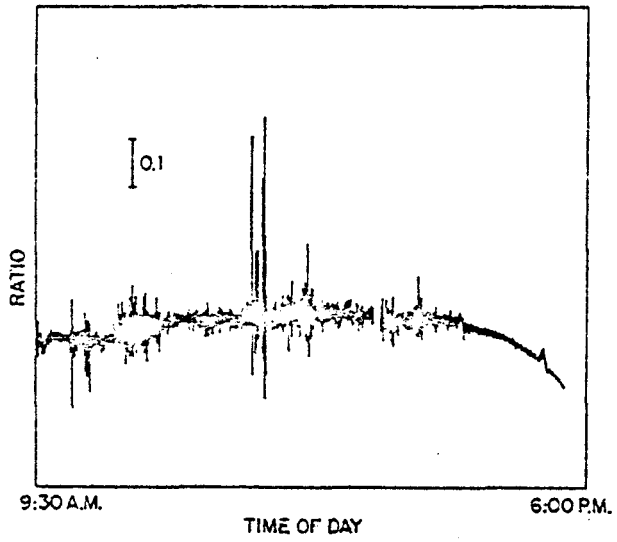

Fig. 3 Ratio of short circuit currents for a GaAs solar cell (E_g = 1.425eV) and an InGaAsP photodiode (E_g = 1.13 eV) vs time of day (March 1978)

Materials requirements for multigap solar cells are very stringent if any real increase in efficiency is ever to be achieved. Each cell must be able to individually operate near its maximum efficiency. So at least for initial choices, because of their state of development, Si, possibly Ge, and III-V binary compounds or alloys are considered the most suitable materials. In general, operation of any solar cell at high levels of illumination requires a non-absorbing lattice-matched window layer on top of each p-n junction; its function is to reduce both the surface recombination velocity which occurs at the photon absorbing surface and the sheet resistance (3). Windows can either be thick or very thin direct bandgap materials, depending upon their bandgap, or thicker indirect material with negligible absorption. Of the two, indirect window materials afford the greater latitude in device fabrication.

Potential solar cell materials are shown in Fig. 4 where their bandgap versus lattice parameter are plotted as an aid to visualizing potential alloy combinations which may prove useful for stacked cell arrangements. In III-V systems, the minority carrier diffusion lengths are only several microns in length. Consequently, p-n junctions must be formed near the surface from materials with absorption coefficients $\gtrsim 10^4$ cm^{-1}. A direct bandgap material must be used then if light is to be absorbed near the junction. The range of direct bandgaps necessary for two or three junction operations is contained within the alloys shown in Fig. 4. The shaded area in the upper portion in Fig. 4 represents the region of indirect absorption of most interest for window layers. For Si, indirect absor-

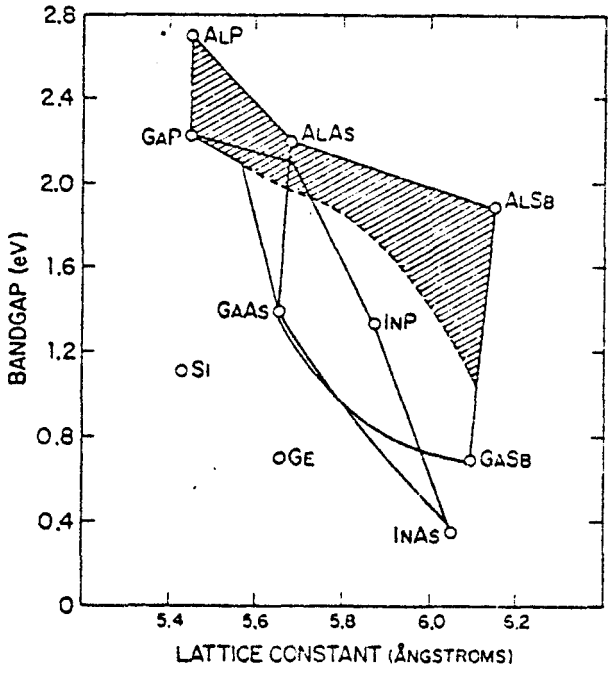

Fig. 4 Bandgap vs lattice constant for potential multigap solar cells. The shaded portion represents indirect bandgap alloys.

ption occurs and intrinsic lifetimes are $\sim 10^3$ times higher. The problems here are maintenance of the lifetime during processing and the lack of a lattice-matched window layer.

Table I lists some possible materials that have a reasonable potential for successfully forming a high efficiency two-bandgap solar cell.

TABLE I

0.7eV	1.1eV	1.4eV	1.7eV
Ge	Si	GaAs	$Al_xGa_{1-x}As$
GaSb	$In_xGa_{1-x}As$		$GaAs_{1-x}P_x$
	$GaAs_{1-x}Sb_x$		$Al_yGa_{1-y}As_{1-x}Sb_x$
	$Ga_yIn_{1-y}As_{1-x}P_x$		
	$Al_yGa_{1-y}As_{1-x}Sb_x$		

Examination of Table I shows that AlGaAs and Si, two highly developed materials, can be combined for maximum efficiency. With only a small penalty in efficiency, Ge and GaAs or GaSb and GaAs can also be combined for maximum efficiency. Except for Si and Ge, use of appropriate window layers is assumed.

INDIVIDUAL CELL FABRICATION AND PERFORMANCE

Individual solar cell performance has been divided into two categories: those that require a substantial lattice constant change from the substrate for the correct alloy formation and those that do not. In the latter category Si and $Al_xGa_{1-x}As$ for $x < 0.25$ have been investigated as solar cells applicable to a spectral splitting approach. $GaAs_{1-x}P_x$ and $GaAs_{1-x}Sb_x$ are the lattice mismatch materials examined, with an eye towards stacked cell applications.

Solar Cells for Spectral-Splitting

Silicon and $Al_xGa_{1-x}As$ ($E_g \geq 1.7$ eV) have been fabricated into concentrator solar cells with an active area of $0.56cm^2$. The contact grid, which covers $\sim 10\%$ of the cell area, is a pattern which had previously been optimized for concentrator AlGaAs/GaAs solar cell operation (9).

The AlGaAs cell, consisting of $p\text{-}Al_{0.92}Ga_{0.08}As/n\text{-}Al_xGa_{1-x}As/n\text{-}GaAs(111)B$ substrate with $x < 0.24$, has been fabricated by LPE in the same manner that is used for conventional AlGaAs/GaAs solar cell and has been reported in detail recently (11). Doping densities in the $n\text{-}Al_xGa_{1-x}As$ layer are $5x10^{17}$ cm^{-3}, while in the p-type $Al_{0.92}Ga_{.08}As$ they are estimated to be $3\text{-}5x10^{18}$ cm^{-3}. Contact resistance of the metal/GaAs/$Al_{.92}Ga_{.08}As$ combination is estimated $\sim 1x10^{-4}$ ohm-cm.

Silicon cells have been designed for operation at photon energies < 1.65 eV and for concentrated sunlight illumination. Because performance at long wavelengths in concentrated sunlight is the primary requirement, junction depths of ~ 1 μm have been used in order to reduce series resistance of the uppermost layer. Obtaining sufficiently high minority carrier lifetimes in the completed cell, a problem often encountered during Si solar cell processing, is aided by starting with Si that has a 500-600 Ω-cm resistivity and reputed 3000-6000 μsec lifetime. In concentrated sunlight, operation is under high injection conditions and the carrier density is maintained by photogenerated carriers. In this case cell polarity is important because the Dember voltage generated is the same polarity regardless of whether the base is p or n type (12). For Si, in which the electron to hole diffusivity ratio is ~ 3, a higher V_{OC} is expected from a p^+-n cell than from a n^+-p cell (13).

Si cells, (p^+;n-;n^+) have been formed by B and P diffusion at $\sim 1200°C$ into a 250 μm thick substrate. Contact resistance after metallization is $< 1 \times 10^{-5}$ ohm-cm^2. Lifetime measurements made by observing the transient decay of V_{OC} after removing a high forward bias have indicated lifetimes of 147 μsec (14). These correspond to an ambipolar diffusion length of 513 μm, about twice the wafer thickness.

Spectral response curves for completed cells with Si_3N_4 anti-reflection coatings are shown in Fig. 5 where response from an AlGaAs/GaAs cell has been included for comparison. Since correction for the contact obscuration has not been made, the actual quantum efficiencies are < 90%. The bandgap of the $Al_xGa_{1-x}As$ is ~ 1.7 eV or $X = 0.24$. A decrease in response for the GaAs and AlGaAs cells at photon energies > 2.3 eV are in large part caused by the one layer A.R. coating having an increasing value of reflectivity at these energies. Silicon on the other hand shows a level response to 1.4 eV above which the expected surface recombination effects as well as increasing reflectivity cause a decrease in response with increasing photon energies.

Performance in concentrated sunlight for AlGaAs (1.61 eV) and Si cells are shown in the I-V curves of Figs. 6 and 7, respectively. In addition, Table II summarizes the important operating parameters.

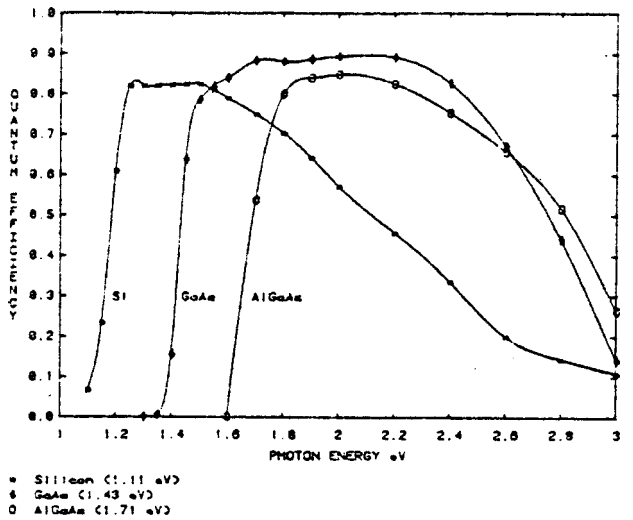

Fig. 5 Spectral response of completed Si, GaAs, and AlGaAs solar cells. Quantum efficiency is not corrected for 10% contact obscuration. Area = 0.56 cm^2.

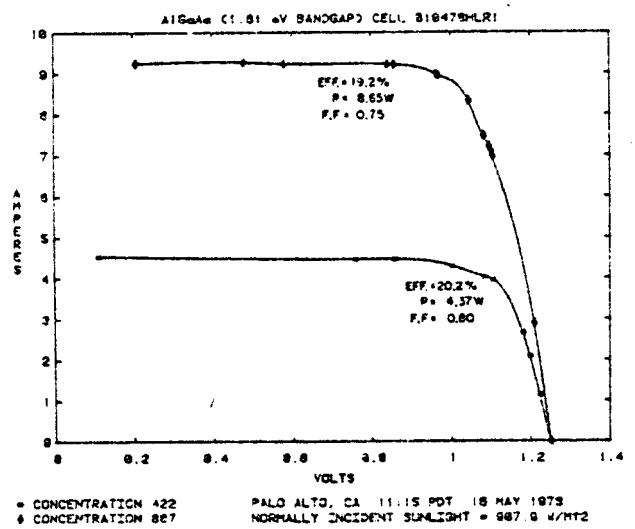

Fig. 6 Current-voltage curves for an AlGaAs (1.6 eV) solar cell operated with illuminating fluxes of 422 and 887 suns.

TABLE II

Solar Cell	Concentration or Current ratio	I_{sc} (Amp)	V_{oc} (Volts)	P_m Watts	Fill Factor	Efficiency Percent
AlGaAs	422	4.54	1.247	4.37	0.80	20.2
	887	9.33	1.259	8.69	0.74	19.2
Si	90.3	1.37	0.709	0.75	0.77	16.0
	178	[a] 2.72	0.722	1.41	0.72	15.2
	406	6.18	0.733	2.85	0.63	13.4
	701	10.86[a]	0.731	4.32	0.55	11.8

[a] the maximum current measured was 10.86A; this may not be I_{sc} as can be seen in Fig. 7.

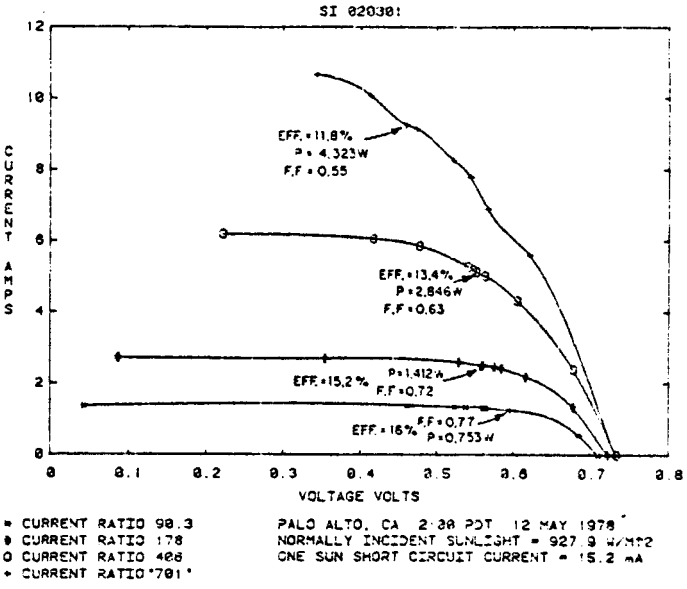

Fig. 7 Current-voltage curves for a Si cell operated under concentrated sunlight.

The AlGaAs cell shows a decrease in fill factor on increasing concentration suggestive of increasing series resistance. The maximum efficiency for a 1.6 eV cell is projected to be ~ 21% at 1000 AM2 suns. The fill factor would then be expected to be 0.84.

Silicon cells that rely upon the carrier density to be photogenerated may experience lifetime improvement with increasing illumination intensity (15). For that reason, the spectral response may change and the short circuit current ratio may not be the concentration ratio. Performance appears limited by a series resistance problem as reflected in the decreasing fill factors. The high series resistance is likely caused by the resistance in the emitter region. Comparison of V_{oc} from this cell to that predicted for a p^+-n shows near perfect agreement with predicted values (13). Since the cell's thickness is 250 μm, very little effect of the n/n^+ contact is expected (16). A further increase in V_{oc} to 0.78 is expected if the base region is reduced in thickness to take advantage of the p^+-n-n^+ configuration of a BSF cell (17).

Alloy Solar Cells for Stacked Cells

Solar cells formed in an alloy in which the composition results in a substantially change in lattice parameter from that of the substrate on which it is grown form another class of cells. Two such alloys have been examined, one is

the AlGaAsP/GaAsP (1.61 eV) grown on a GaP(111)B substrate and the other is AlGaAsSb/GaAsSb (1.15 eV) grown on GaAs (111)A substrate. The mismatch is $\sim$ 1.7% and 1.3%, respectively. Formation of each cell required the continuous lattice constant grading from the substrate to the final alloy composition. Both cells are in an Al-Ga-column V alloy system where the lattice parameter is dictated by the column V sublattice composition. Once the correct composition has been achieved, increasing the bandgap simply occurs by Al addition.

The advantage of the GaAsP system is that a 1.65 eV cell can be formed on a substrate of GaP which is transparent to photons < 2.25 eV. Thus, the unused photons (< 1.65 eV) are transmitted directly through the substrate in contrast to the AlGaAs cell grown on GaAs with E_g = 1.43 eV. A potential reduction in optical complexity can then be envisaged.

On the other hand, the AlGaAsSb system possesses the unique distinction that a complete stacked cell is possible within its phase boundaries. Both the lower 1.1 eV and the upper 1.65 eV junctions with window layers can be deposited at single lattice constant. Only Al additions are necessary for increasing the bandgap from $GaAs_{0.84}Sb_{0.16}$ (1.15 eV) to the $Al_yGa_{1-y}As_{0.84}Sb_{0.16}$ (1.65 eV) composition and finally to the top window layer. The maximum Al concentration that has been observed in the $Al_yGa_{1-y}As_{0.84}Sb_{0.16}$ alloy is y = 0.88, a composition which corresponds to a 2.05 eV indirect bandgap (18). Thus, all necessary compositions are attainable for a stacked cell formation in this system.

Lattice constant grading by liquid phase epitaxy (LPE) for the GaAsP cell utilized P depletion from a Ga-As-P solution to first deposit n-GaP layer on n-GaP(111)B substrate and then as the temperature is lowered to gradually change composition to n-GaAsP. The cooling interval is between 1000 and 800C. Once the GaAsP composition is reached a p-AlGaAsP layer is deposited and diffusion of the p-type dopant into n-type layer forms the p/n junction. For the Sb containing alloy, compositional grading is attained by Al depletion which lowers the As activity as growth proceeds between 830°C and 770°C from an Al-Ga-As-Sb solution. Once the correct lattice constant is reached, depositions of n-GaAsSb followed by p-AlGaAsSb takes place. Again junction formation is by p-diffusion during LPE into the n-type ternary.

Spectral response curves from preliminary cells grown in both systems are shown in Fig. 8. Immediately obvious is the lower overall yield caused by the lack of an A. R. coating, but more importantly, the behavior or shape indicative of low n-type diffusion length.

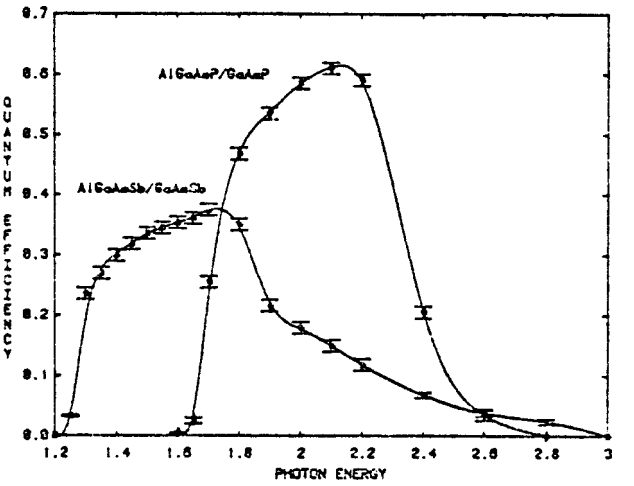

Fig. 8 Spectral response curves for solar cells composed of p-AlGaAsP/p-nGaAsP/graded GaAsP/GaP(111)B substrate and p-AlGaAsSb/p-nGaAsSb/graded AlGaAsSb/GaAs(111)A substrate.

The cause for diffusion length $\lesssim$ 0.5 µm is not yet known. Possibilities being investigated are: (1) grading effects associated with high dislocation densities, (2) unusual stoichiometric conditions that may cause more non-radiative centers and traps, and (3) a compositional variation that may cause bandgap dips in the junction vicinity. Open circuit voltages of 1.1V and $\sim$ 0.48V at low current densities produced by a tungsten lamp have been observed for GaAsP and GaAsSb, respectively.

TWO CELL PERFORMANCE

Operation of Si and AlGaAs in a two cell configuration requires a dielectic mirror as a means of spectral splitting with the crossover between the stopband and passband region near 1.65 eV. With a two-cell configuration, reflection of the light to either the low bandgap or the high bandgap cell is possible. The proper choice is to reflect light to the low bandgap cell and to let light pass through the filter to the high bandgap cell for the following reasons:

1) It is easier to obtain nearly 100% reflectivity over the desired stopband than it is to obtain zero reflectivity over a desired passband. If the low bandgap cell were constructed so that its window layer still passed light with photon energies above the bandgap of the high bandgap cell, then any reflected light outside the reflection stopband is still utilized to produce photocurrent. With the alternate configuration this reflected light is wasted.

2) The high bandgap cell is more tolerant of temperature increases than the low bandgap cell. So with the preferred configuration most of the very long wavelength radiation which produces only heat is incident on the high bandgap cell.

Although selective mirrors are commercially available it has been found advantageous to perform a computer design of the filter which can include the optical behavior of the antireflection coatings of each cell. With such a program the effect on total performance of any small changes in layer thickness of every layer in the stack can be examined. Using such a procedure a 17 layer (quarter-wave stack with eighth-wave ends) dielectric filter of alternating ZnS and Na_3AlF_6 has been designed and fabricated for 22° angle incidence. The designed reflectance vs. photon energy is shown in Fig. 9. Experimentally a rise in reflectance above the design value at higher photon energies is noted (not shown) and is believed to be caused by slight errors in the refractive indice values in the calculation.

When the dielectric filter is combined with concentrator cells of Si and AlGaAs in a single concentrator mount the spectral response shown in Fig. 10 is observed. In this arrangement Si shows a nearly optimum quantum efficiency curve with the higher energy photons which would be converted with lower efficiency, being directed onto the AlGaAs cell. The advantage of reflecting onto the low bandgap cell is apparent where photons >1.65 eV not incident upon the AlGaAs cell are still seen to give response in Si.

Operation in concentrated sunlight produces the current-voltage curves of Fig. 11. The total power output with both cells operating at their maximum efficiency points is 2.355 watts with an effective intensity of 165 suns on the cells, and an AM 1.23 spectrum. The subsystem conversion efficiency under those conditions is 28.5%; the operating characteristic of each cell is tabulated in Table III. Given a perfect filter, the combined efficiency would be approximately 31%.

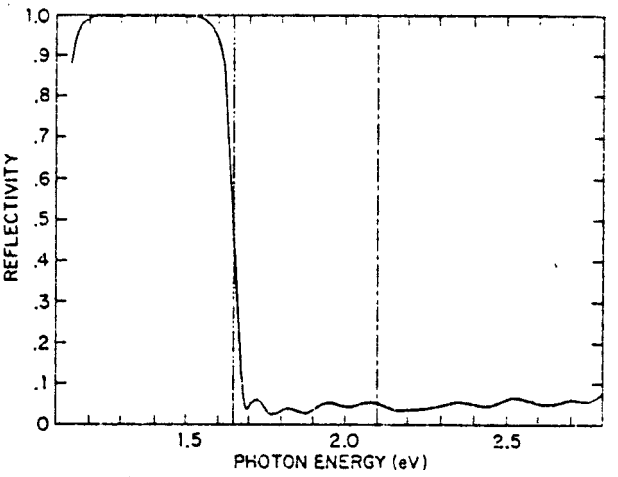

Fig. 9 Computed response of a 17-layer dielectric mirror formed with alternating ZnS (n=2.3) and Na_3AlF_6 (n=1.35).

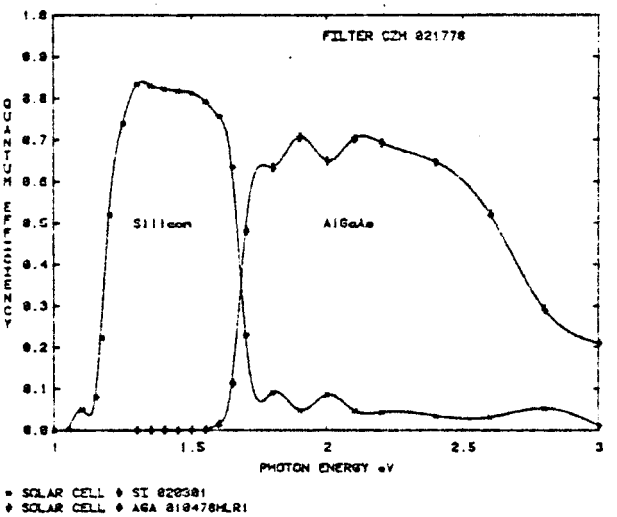

Fig. 10 Spectral response of a Si and AlGaAs concentrator cells mounted with a spectral splitting filter. Each cell is 0.56 cm^2 in area.

TABLE III

Cell	I_{sc} (Amp)	V_{oc} (Volts)	P_m (Watts)	Fill Factor	Efficiency Percent
AlGaAs (1.61 eV)	1.382	1.26	1.440	0.827	17.4
Si (1.1 eV)	1.711	0.738	0.915	0.725	11.1

Allowing for losses in the concentrator optics and filter, the system efficiency is estimated to be in the neighborhood of 25%. By reducing the current from the Si cell from 1.5 to 1.3 amps (with a corresponding increase in voltage and very little penalty in efficiency) the two cells could be operated in series to generate just under 1.8 volts and 1.3 amps, or very nearly the maximum power for the two independent cells.

This represents a preliminary experiment on cells which have a contact grid optimized for an AlGaAs/GaAs solar cell designed to operate at 1000 suns. In spectral splitting each cell operates at a lower current than if it were used alone at the same concentration. Improved performance is expected from a reduction of contact obscuration when an optimized grid is used. This together with an improved filter design, is expected to produce further performance enhancements.

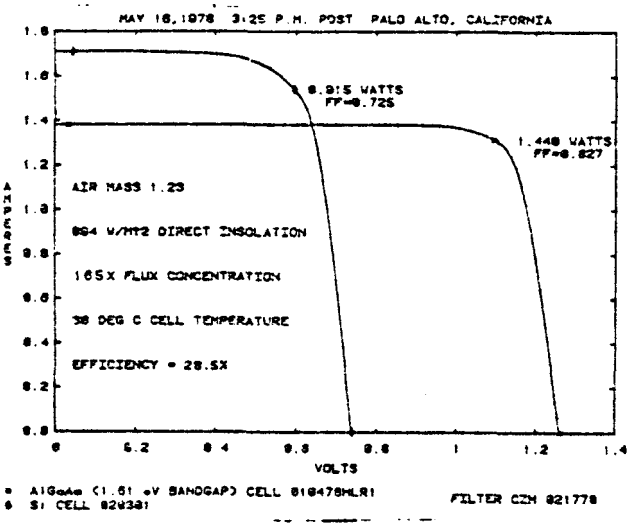

Fig. 11 Current-voltage curves for Si and AlGaAs in a spectral splitting arrangement, operating in concentrated sunlight.

SUMMARY AND CONCLUSIONS

Efficiency estimates for a multigap solar cell with two junctions yield a maximum value of ∿ 33% for 1000 suns at AM2 and 30°C. Optimum bandgaps for short circuit current equality in each cell are 1.1 and 1.65eV. Shifting the bandgaps to 0.7 and 1.4eV would yield an efficiency of 31%.

The short circuit equality condition for design is shown to be near the maximum efficiency seen when two cells are considered to be operated independently. So, little efficiency loss is encountered when this condition is used for optimization. Very preliminary data suggest that the ratio of short circuit currents from 1.1eV and 1.4eV cells show little diurnal variation except near sunset and during cloudy periods. Additional data of this nature and over a greater range in photon energies is needed.

For two or three bandgap concentrator cells Si, Ge, and compounds or alloys in the Al-Ga-As, Al-Ga-As-P and Al-Ga-As-Sb systems are potential meterials which are either highly developed or reasonably well understood. The Al-Ga-As-Sb system is unique in that all the necessary bandgaps for a two bandgap cell occur at a single lattice constant value. Cells showing near projected performance are those which do not require a change in lattice parameter from that of the substrate in order to obtain the correct composition.

Solar cells formed in AlGaAs (1.6leV) have demonstrated efficiences > 19% at concentrations ≤ 887 suns, with only a small change in fill factor with higher illumination. Silicon cells designed for operation in concentrated sunlight show a maximum efficiency of 16% at current ratios of 90, but decrease in efficiency to 12% as the current ratio reaches 700. Although useful for low illumination fluxes, the expected behavior at high fluxes again points to the need for a low bandgap cell that also has a lattice-matched window layer which would reduce sheet resistance. This is absolutely necessary if both high efficiency and high power are to be expected from a two bandgap cell arrangement. Preliminary attempts in this direction using AlGaAsSb/GaAsSb (1.15eV) demonstrate the feasibility of this cell. Although low minority carrier diffusion lengths presently hinder its deployment, materials investigations are in their early stages, and improvements are expected as new insights are gained.

A two-cell arrangement using cells of Si and AlGaAs and a dielectric mirror has achieved a conversion efficiency of 28.5% for the two cells operated at 165 suns at AM 1.23. This has demonstrated the viability of the multigap concept and suggests that both materials and optical developments can lead to higher efficiencies and power levels.

ACKNOWLEDGEMENTS

The authors wish to thank R. L. Bell for his continued support and T. Boyle, D. D. Weber, S. Hikido, A. L. Ollerdessen, K. E. von Dessoneck, B. Oxley, and R. Fulks for experimental assistance. Also the support by Sandia Laboratories under Contract #07-6953 and by The Division of Basic Energy Sciences of the Department of Energy Contract EY-76-C-03-1250 is greatly appreciated.

REFERENCES

1. E. D. Jackson, Trans. Conf. on the Use of Solar Energy, Tucson 1955, U. of Arizona Press, Tucson, Vol.5, p. 122-126, 1958.

2. L. W. James and R. L. Moon, APL 26, (1975) p. 467.

3. L. W. James and R. L. Moon, 11th IEEE Photovoltaic Specialists Conf. (1975) May 6-8, 1975, p.402.

4. R. Davis and J. R. Knight, Sol. Energy 17 (1975) p. 145.

5. L. W. James, Int'l. Electr. Device Meeting, Washington,D.C., Dec. 1975, p.87.

6. J. J. Loferski, 12th IEEE Photovoltaic Specialists Conf. (1976) p.957, Baton Rouge.

7. N. S. Alvi, C. E. Backus, G. W. Masden, 12th IEEE Photovoltaic Specialists Conf. (1976) p.948, Baton Rouge.

8. E. A. DeMeo and P. B. Bos, ER-589-SR, Jan. 1978, Electric Power Research Institute, Palo Alto, CA.

9. H. A. Vander Plas, L. W. James and R. L. Moon, 13th IEEE Photovoltaic Specialist Conf., Washington, D.C. 1978. See also L. W. James, H. A. Vander Plas and R. L. Moon, Final Report Sandia Laboratories Contract #05-4413.

10. M. Wolf, Energy Conversion, 11 (1971) p.63.

11. R. L. Moon, L. W. James, H. A. Vander Plas and N. J. Nelson, to be published Appl. Phys. Letters.

12. H. Dember, Physik Z. 32 (1931) p.554.

13. J. G. Fossum and F. A. Lindholm, IEEE Trans. on Electr. Devices, ED-24 (1977) p.325.

14. S. C. Choo and R. G. Mazur, Solid State Electr. 13 (1970) p.553.

15. W. Zimmerman, Electronic Letters, 9 (1973) p.378.

16. H. J. Hovel, Ed. Willardson & Beer, Semiconductors and Semimetals, Vol.11 Acad. Press 1975, p.96.

17. J. G. Fossum, F. A. Lindhohm and E. L. Burgess, Proc. DOE Photovoltaic Concentrator Systems Workshop. Scottsdale, Az, May 2426, 1977, p.23.

18. R. L. Moon, Progress Report #2, May 1978, DOE Contract No. EY-76-C-03-1250, Basic Energy Sciences Div.

19. H. A. Macleod, Thin-Film Optical Filters, American Elsevier Pub. Co. Inc., New York 1969.

ty N_D in the different samples was determined from low-temperature capacitance-voltage measurements and are also listed in Table I.

The density N_T of the traps in the OMVPE samples with different ratios of As to Ga was determined from the capacitance transients using the relation[8]

$$N_T = N_D\,[(C_\infty/C_0)^2 - 1\,], \tag{2}$$

which is valid for the large value of quiescent reverse bias applied to the barrier during the measurements. C_0 and C_∞ are, respectively, the values of the depletion layer capacitance at $t = 0$ and ∞. The value of N_T for the dominant 0.82 ± 0.02-eV electron trap was also determined from [9]:

$$N_T = \frac{2N_D\tau_n}{C_0}\left(\frac{dC}{dt}\right)_0\left(\frac{\lambda_0}{W_0}\right)^2, \tag{3}$$

where W_0 is the depletion layer width at $t = 0$, and λ_0 is the distance from the metal-semiconductor interface at $t = 0$ where the Fermi level intercepts the electron trap level for the quiescent reverse bias applied to the diode. The values of N_T for the 0.82 ± 0.02-eV electron trap determined from capacitance-voltage measurements and from Eqs. (2) and (3) were found to be in good agreement. These values are listed in Table I and are plotted in Fig. 3 as a function of the As to Ga ratio.

The most significant result obtained from the present investigation is that the 0.83-eV electron trap commonly observed in conventional VPE GaAs is also present in OMVPE GaAs with an identical capture cross section and that its concentration increases linearly with the As/Ga ratio in the crystal. This indicates the involvement of V_{Ga} or a chemical impurity associated substitutionally or interstitially with a Ga site in the formation of the center. An antisite defect As_{Ga} is also a possibility. Miller *et al.*[10] have also reported that the density of the 0.82-eV level in VPE GaAs increased with increasing AsH_3 to GaCl ratio during growth. In fact, the values of N_T determined by these authors in GaAs with As/Ga ratios of 1 and 3 are in excellent agreement with our results and are shown in Fig. 3. It is unlikely that the impurity is oxygen on a substitutional or interstitial site, since the absence of HCl in the OMVPE process precludes the formation of oxygen by the dissociation of silica. However, oxygen containing compounds may be present in the sources, particularly AsH_3. By a comparison between quantitative oxygen concentration and the electron trap concentration in bulk GaAs material, it has been shown recently by Huber *et al.*[11] that oxygen is not involved, either directly or as part of a complex defect, in the origin of the 0.82 ± 0.02-eV level. Furthermore, theoretical studies[12,13] also suggest that this deep state is not related to oxygen.

The 0.36 ± 0.02-eV electron trap identified in samples OM 490, 489, and 330 as indicated in Fig. 1 has been sometimes observed in as-grown and heat-treated VPE GaAs.[5] Comparing these data with the data by Martin *et al.*,[1] it may, however, be concluded that the trap level observed by us is not the trap labelled EL5 ($\Delta E_T = 0.42$ eV), which anneals out by heat treatment and has a value of σ_∞ two orders of magnitude higher than we observe. It is also not identical to the level labelled EL7 for which the values of τ_n are very different. This center, being reported possibly for the first time, is attributed to an unknown impurity and will be investigated further.

The 0.35-eV hole trap observed in OMVPE 329 might be due to Fe impurities since Fe contamination is usually present in TMG, typically to the extent of a ppm or so. However, the Fe compounds are not likely to be very volatile and Fe normally produces a hole trap approximately 0.5 eV above the valence band. The 0.31-eV hole trap observed in OMVPE 317 is ascribed to unknown impurities.

We wish to thank R.L. Bell for his support and interest, G.A. Antypas for providing the GaAs substrates, S. Fonte for technical assistance, and S.H. Chiao for his interest in the work. Helpful discussions with D.V. Lang, R.N. Bhargava, and M. Ettenberg are gratefully acknowledged. One of us (J.W.K.) thank the Department of Electrical and Computer Engineering, OSU, for financial assistance.

[1] G.M. Martin, A. Mintonneau, and A. Mircea, Electron. Lett. **13**, 191 (1977).
[2] A. Mitonneau, G.M. Martin, and A. Mircea, Electron. Lett. **13**, 666 (1977).
[3] S.J. Bass, J. Cryst. Growth **31**, 172 (1975).
[4] A.M. White, P.J. Dean, and P. Porteous, J. Appl. Phys. **47**, 3230 (1976).
[5] P.K. Bhattacharya, Ph.D. thesis, University of Sheffield, United Kingdom, (1978).
[6] A. Majerfeld and P.K. Bhattacharya, Appl. Phys. Lett. **33**, 259 (1978).
[7] J.A. Van Vechten and C.D. Thurmond, Phys. Rev. B **14**, 3539 (1976).
[8] M. Bleicher and E. Lange, Solid State Electron. **16**, 375 (1973).
[9] P.K. Bhattacharya, S.J.T. Owen, and J. Marrs (unpublished).
[10] M.D. Miller, G.H. Olsen, and M. Ettenburg, Appl. Phys. Lett. **31**, 538 (1977).
[11] A.M. Huber, N.T. Linh, M. Valladon, J.L. Debrun, G.M. Martin, A. Mitonneau, and A. Mircea, J. Appl. Phys. **50**, 4022 (1979).
[12] M. Jaros, Phys. Rev. B **16**, 3694 (1977).
[13] A. Mircea, A. Mitonneau, J. Hallais, and M. Jaros, Phys. Rev. B **16**, 3665 (1977).

*THE ORGANOMETALLIC VPE GROWTH OF $GaAs_{1-y}Sb_y$ USING TRIMETHYLANTIMONY AND $Ga_{1-x}In_xAs$ USING TRIMETHYLARSENIC

C. B. Cooper III, M. J. Ludowise, V. Aebi, and R. L. Moon

Corporate Solid State Laboratory
Varian Associates, Inc.
Palo Alto, CA 94303

(Received September 10, 1979; revised November 26, 1979)

The organometallic vapor phase epitaxial growth of $Ga_{1-x}In_xAs$ and $GaAs_{1-y}Sb_y$ using trimethylarsenic and trimethylantimony as the Group V sources is reported and the relevant chemistry is discussed. Growth rate and composition variations as a function of temperature are given for $GaAs_{1-y}Sb_y$. A result of particular importance is that no detrimental room temperature gas phase reaction is observed between triethylindium and trimethylarsenic. Consequently, the growths are performed at one atmosphere pressure without the need for any complicated injection schemes in the reactor design.

Key words: organometallic vapor phase epitaxy, GaInAs GaAsSb, trimethylarsenic, trimethylantimony.

*This work was supported by the U.S. Dept. of Energy. First, the concept of III-V growth using column V trialkyls was verified using TMSb for the growth of GaAsSb under Contract No. EY-76-C-03-1250 from the Div. of Materials Sciences Branch of the Office of Basic Energy Sciences. After successful verification, TMAs was tried for the growth of InGaAs, which is supported by the Solar Energy Research Institute under Contract No. XP-9-8081-1.

0361-5235/80/0300-0299$03.00/1 © 1980 AIME

Introduction

Organometallic vapor phase epitaxy (OM-VPE) is rapidly becoming a popular method for the growth of III-V semiconducting compounds (1-5). In particular, GaInAs has been investigated for fiber optic sources (6) and detectors (7), low bandgap solar cells (8), and photocathodes (9), and GaAsSb may find application in fiber optics (10,11) and superlattice devices (12). Most authors report the use of the Group III trialkyls [trimethylgallium (TMGa), trimethylaluminum (TMAl) and triethylindium (TEIn)] as the column III source and the Group V trihydrides AsH_3, PH_3, and SbH_3 as the column V sources. Thomas reported the use of triethylphosphorous in GaP growth (13) and Manasevit mentions the use of trimethylantimony (TMSb) to grow GaAsSb, but no details are given (14). In general, however, little attention has been given to the advantages of using the column V trialkyls instead of the trihydrides as the Group V sources.

The column V trialkyls offer distinct advantages over the trihydrides for the growth of In-V and III-Sb alloys. In the case of In containing alloys, TEIn is generally used in combination with AsH_3 or PH_3 (15-18). These combinations present difficulties owing to a rapid room temperature reaction which rapidly depletes the TEIn from the carrier gas upstream of the substrate wafer (17,18). Noad and Springthorpe recently reported GaInAs growth using a technique which physically separates the TEIn + TMGa mix from the AsH_3 until just before the gas stream reaches the substrate, however, large amounts of TEIn were still consumed in the gas phase reaction (17). Other authors report InP and GaAs growth at low pressure (18), but this requires more cumbersome equipment than growths done at one atmosphere. The use of trimethylarsenic (TMAs) as the column V carrier prevents the gas phase reaction thereby allowing growths in conventional OM-VPE reactors (19) at atmospheric pressure.

The growth of III-Sb compounds is simplified in OM-VPE reactors by the use of TMSb rather than SbH_3, which is difficult to handle (20). It should also be noted that OM-VPE has an inherent advantage over HCl transport VPE (21,22) for growing the antimonides owing to the fact that higher Sb concentrations may be obtained in the gas phase allowing higher growth rates and more uniform growths of GaSb and GaInSb (23).

corresponding gallium or aluminum compounds is well known (27). By using TMAs rather than AsH_3 to grow GaInAs, the elimination reaction is thus avoided allowing transport of the TEIn, either singly or as a Lewis acid-base complex.

Experimental

The epitaxial layers of this work are grown in an RF induction heated horizontal cold wall reactor similar to that described by Bass (19). The Ga and In sources are electronic grade TMGa and TEIn (supplied by Alfa or Texas Alkyls), and the Group V sources are AsH_3 (10% in H_2, Scientific Gas Products, Inc, Santa Clara, CA), TMAs (Alfa) and TMSb (Alfa). Palladium diffused H_2 is used as the carrier gas and normally is at a flowrate of 10 slpm. The substrates are single crystal GaAs doped with Sn or Cr and are oriented 2° toward (110) from the (100) plane.

Growth temperatures for GaInAs are usually near 600°C. Typical mole fractions in the reactor for GaInAs are 8.4×10^{-5} and 8.4×10^{-4} for column III and V, respectively; and for GaAsSb column III and column V are 1.5×10^{-4} and 2.1×10^{-4}.

The growth begins by heating the susceptor and wafer under flowing AsH_3 until the growth temperature is reached. For the GaInAs growths, the TMAs flow is started after stabilization at the growth temperature and the AsH_3 flow is stopped. The reactor is purged under these conditions for 5 min. and then growth is begun. For the GaAsSb growths, TMGa and TMSb flows are started simultaneously without interrupting the AsH_3 flow. Growths are typically 20 to 60 min. in length.

The $Ga_{1-x}In_xAs$ solid compositions are measured by photoluminescence (PL) (28) and the $GaAs_{1-y}Sb_y$ compositions are measured by a combination of PL (29) and X-ray lattice constant measurements. In all cases the GaInAs PL signal was strong enough and the peaks sharp enough to firmly establish the composition. In the case of GaAsSb, PL and X-ray lattice constant data were used since the PL data was not always of sufficient quality to unambiguously establish the composition. The error bars in Fig. 4 reflect the discrepancy between the two techniques.

Chemistry

The Group III alkyls, MR_3, (where M = Al, Ga, In; R = alkyl) are an electron deficient class of compounds called Lewis acids whereas the Group V hydrides and alkyls, ER'_3, (where E = N, P, As, Sb; R' = H, alkyl) are Lewis bases or electron rich species (24). Reactions between these classes of compounds to form Lewis acid-base complexes (Eq. 1) are well known, and are represented by the equation

$$MR_3 + ER'_3 \longrightarrow R_3MER'_3 \qquad (1)$$

Despite the relatively weak nature of the donor-acceptor bond, many complexes have been isolated and characterized (25,26).

In most OM-VPE reactors hydrogen streams containing the Group III and V sources are mixed and then passed over a heated substrate. It might, in general, be expected that the gas stream would become depleted of reactants owing to the formation of Lewis acid-base complexes, since the complexes usually have vapor pressures which are much lower than the source organometallics. This is avoided in OM-VPE systems by keeping the mole fractions of the reactants low ($\sim 10^{-3}$) and by maintaining relatively high gas velocities. If, however, the Lewis acid-base complex readily undergoes further reaction to form a less volatile product, depletion of the reactants may occur. For example, when the Group V source contains an active hydrogen, the complex may undergo hydrocarbon elimination (27) according to Eq. (2).

$$R_3MEH_2R' \longrightarrow \text{polymeric solid} + RH \qquad (2)$$

The solid products usually have a high melting point and very low vapor pressure consistent with a polymeric species. The elimination reaction can be prevented if the Group V compound does not contain a readily available hydrogen. The reaction of $As(CH_3)_3$ with InR_3, for instance, is expected to give a Lewis acid-base complex which does not undergo hydrocarbon elimination. The growth of GaInAs from indium alkyls has been complicated in the past by a low temperature gas phase reaction between the indium species and arsine, probably according to Eq. (2). This is not surprising since the tendency for indium containing Lewis acid-base complexes to undergo elimination reactions more readily than the

The growth of $GaAs_{1-y}Sb_y$ is investigated in more detail. Growths are performed at temperatures ranging from 500 to 630°C using a TMGa:AsH_3:TMSb mole fraction ratio of 2.4:1:2.4. The ratios are kept constant to determine the effect of temperature on growth rate and Sb incorporation in the crystal. Fig. 2 shows the surface morphology of a $GaAs_{1-y}Sb_y$ ($y \sim 0.06$) layer grown directly on a GaAs substrate. Note the cross-hatch pattern typical of lattice mismatched epitaxial layers (30) and the numerous hillocks. The growth rate increases an order of magnitude between 560 and 600°C as shown in Fig. 3. A similar effect has been observed in the growth rate of GaSb and GaInSb on GaSb using TMGa and TMSb (23). Fig. 4 shows the Sb content of the crystal, y, as a function of growth temperature. A gradual decrease in the Sb incorporation is noted from 500°C to 625°C. Above 625°C it is difficult to obtain very high Sb concentrations. These results contrast with an earlier report indicating that a change in growth temperature does not affect the solid composition (20). The growth rate increases markedly above 580°C, but the Sb incorporation decreases abruptly. These changes reflect a kinetic balance between the As and Sb atoms relative to basic atomic incorporation mechanisms such as atomic surface mobility (33). The temperature 580°C may represent the boundary between surface kinetically controlled growth and mass transport limited growth at higher temperatures.

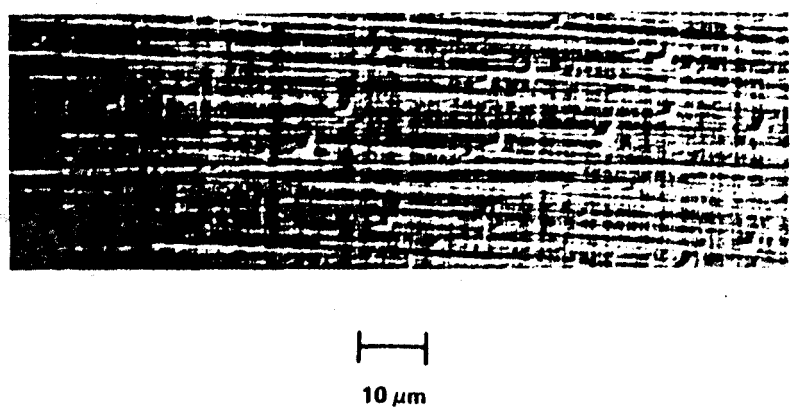

Fig. 2 Surface morphology of an OM-VPE $GaAs_{1-y}Sb_y$ ($y \sim 0.06$) epitaxial layer grown on a GaAs substrate.

Results and Discussion

Fig. 1 shows the surface and cross-section of a $Ga_{1-x}In_xAs$ layer ($x \simeq 0.24$) grown directly on the substrate with no grading layer. The surface is specularly reflective, smooth, generally free from defects, and exhibits the regular crosshatch (30) pattern typical of lattice mismatched epitaxial layers.

A gas phase ratio of [TEIn]/[TEIn + TMGa]$\sim$ 0.29, is used. Here, the TEIn flux assumes a vapor pressure for TEIn at 21°C of 0.12 Torr, but this is not known with any certainty (16,31,32). The growth rate at 600°C under these fluxes is 0.03 μm/min, and drops to 0.017 μm/min at half the above fluxes.

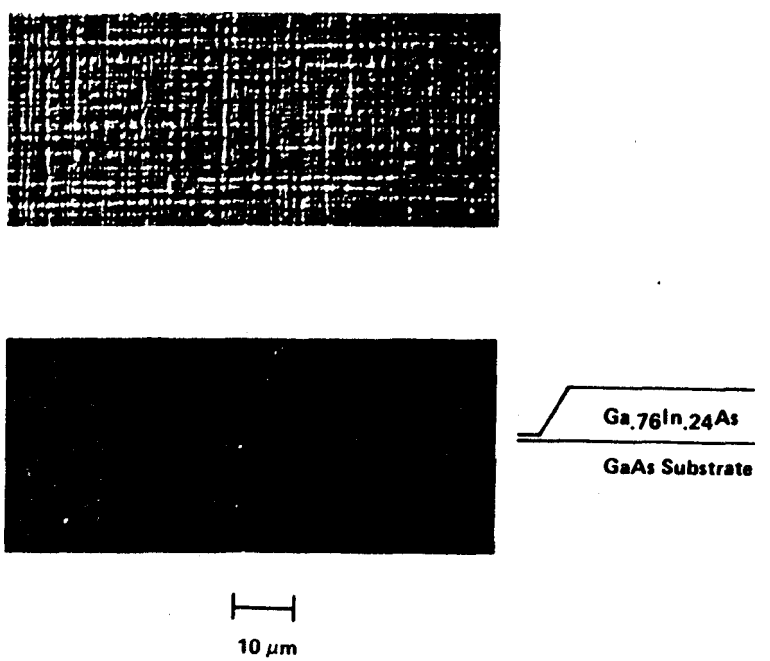

Fig. 1 Surface morphology and cross-section of an OM-VPE $Ga_{1-x}In_xAs$ ($x \sim 0.24$) epitaxial layer grown on a GaAs substrate.

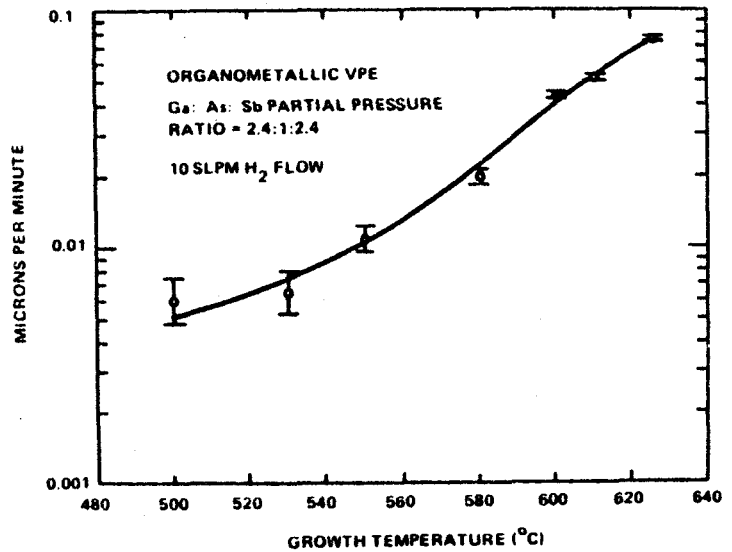

Fig. 3 Growth rate as a function of growth temperature for TMGa:AsH_3:TMSb partial pressure ratio of 2.4:1:2.4.

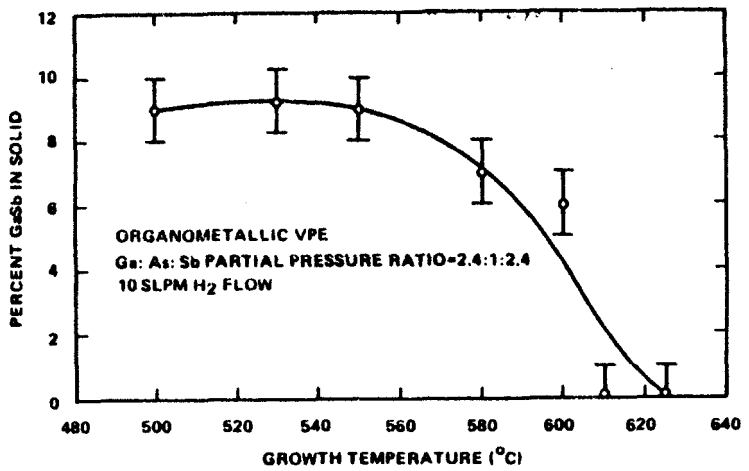

Fig. 4 GaSb fraction in $GaAs_{1-y}Sb_y$ as a function of growth temperature for TMGa:TMAs:TMSb partial pressure ratio of 2.4:1:2.4.

In general, for flux ratios differing from those used in Fig. 3 and 4, it is noted that increasing the AsH_3/TMSb ratio decreases Sb incorporation, as expected, while increasing the TMSb/TMGa ratio results in the appearance of droplets and needles on the wafer surface, probably owing to a vapor-liquid-solid growth mechanism (34).

No indication of a miscibility gap is noted for $0 \leq y \leq 0.11$, contrary to what is expected from the report of Gratton et al. (35) who used solution growth techniques. This correlates with molecular beam epitaxy data (36,37) and indicates that the miscibility gap is in the liquid rather than the solid solution $GaAs_{1-y}Sb_y$.

Conclusions

The column V trialkyls TMAs and TMSb are demonstrated to be useful for the growth of III-V epitaxial layers by OM-VPE, and they have particular advantages in some cases over the column V trihydrides. Single crystal epitaxial layers of $Ga_{1-x}In_xAs$ ($x \leq 0.24$) have been grown by OM-VPE using TMAs as the sole source of As. Particularly important is that, the room temperature gas phase reaction between TEIn and AsH_3 is avoided using a chemical approach rather than physically separating the reactants or resorting to low pressure techniques. Epitaxial layers of $GaAs_{1-y}Sb_y$ are also grown by OM-VPE with $0 \leq y \leq 0.11$ using TMSb as the Sb carrier.

Finally, the absence of a detrimental reaction between TEIn and TMAs suggests that triethylphosphorous or trimethylphosphorus rather than PH_3 might be suitable for use in the growth of InP and InP-related compounds.

Acknowledgements

The authors gratefully acknowledge R. L. Bell for his encouragement and continued support, L. W. James, R. R. Saxena and G. A. Antypas for the GaAs substrates and his unique insights. We thank L. Garbini and J. Bash for X-ray measurements and D. Akselrad, L. G. Mandoli, C. Molinari and J. L. Unruh for expert technical assistance.

References

(1) N. J. Nelson, K. K. Johnson, R. L. Moon, H. A. Vander Plas, and L. W. James, Appl. Phys. Lett. 33, 26 (1978).

(2) H. Morkoc, J. Andrews and V. Aebi, Electron. Lett. 15, 105 (1979).

(3) R. D. Dupuis and P. D. Dapkus, Appl. Phys. Lett. 33, 68 (1978).

(4) G. B. Stringfellow and H. T. Hall, Jr., J. Electron. Mater. 8, 201 (1979).

(5) J. P. Duchemin, M. Bonnet, F. Koelsch, and D. Huyghe, J. Electrochem Soc. 126, 1134 (1979).

(6) B. I. Miller, J. H. Fee, R. J. Martin and P. K. Tien, IEEE Trans. Electron. Dev. ED-24, 1213 (1977).

(7) K. J. Bachmann and J. L. Shay, Appl. Phys. Lett. 32, 446 (1978).

(8) R. R. Saxena and R. L. Moon, to be published.

(9) J. S. Escher, P. E. Gregory, S. B. Hyder and R. Sankaran, J. Appl. Phys. 49, 2591 (1978).

(10) R. C. Eden, Proc. IEEE 63 32 (1975).

(11) A. Y. Cho, H. C. Casey, Jr and P. W. Foy, Appl. Phys. Lett. 30, 397 (1977).

(12) G. A. Sai-Halasz, R. Tsu and L. Esaki, Appl. Phys. Lett. 30, 651 (1977).

(13) R. W. Thomas, J. Electrochem Soc. 116, 1449 (1969).

(14) H. M. Manasevit and W. I. Simpson, J. Electrochem Soc. 116, 1725 (1969).

(15) H. M. Manasevit and W. I. Simpson, J. Electrochem Soc. 120, 135 (1973).

(16) B. J. Baliga and S. K. Ghandi, J. Electrochem. Soc. 122, 683 (1975).

(17) J. P. Noad and A. J. Springthorpe, Paper L-6, 21st Electronic Materials Conference, Boulder Colorado, 1979.

(18) J. P. Duchemin, M. Bonnet, G. Beuchet and F. Koelsch, "Gallium Arsenide and Related Compounds 1978", (Inst. Phys. Conf. Ser. No. 45), pp. 10-18.

(19) S. J. Bass, J. Crystal Growth 31, 172 (1975).

(20) R. B. Clough and J. J. Tietjan, Trans. Soc. AIME 245, 583 (1969).

(21) T. Kiyosawa, K. Masumoto, and S. Isomura, J. Cryst. Growth 30, 317 (1975).

(22) I. Nakatani and K. Masumoto, J. Cryst. Growth 46, 205 (1979).

(23) M. J. Ludowise, unpublished data.

(24) G. E. Coates, M. L. H. Green and K. Wade, "Organometallic Compounds: The Main Group Elements", Vol I, 3rd ed. Meuthen & Co., LTD, London, 1967.

(25) F. G. A. Stone, Chem. Rev., 101 (1958).

(26) G. E. Coates, Jour. Chem. Soc., 2003 (1951).

(27) O. T. Beachley and G. E. Coates, Jour. Chem. Soc., 3241 (1965).

(28) K. R. Schulze, H. Neumann and K. Onger, Phys. Status Solidi (b) 75, 493 (1976).

(29) R. E. Nahory, M. A. Pollack, J. C. DeWinter and K. M. Williams, Appl. Phys. 48, 1607 (1977).

(30) G. H. Olsen and M. Ettenberg in Crystal Growth Theory and Techniques, C. H. L. Goodman (ed.), Plenum Press, New York (1978).

(31) B. J. Baliga, Ph.D. Thesis, 1974, Rensselear Polytechnic Institute, Troy, New York.

(32) C. B. Cooper III, unpublished data.

(33) J. A. Venables and G. L. Price in Epitaxial Growth, J. W. Matthews, ed., Academic Press, N.Y. 1975.

(34) E. I. Givargizov, Curr. Top. Matl. Sci. 1 79 (1978).

(35) M. F. Gratton, R. G. Goodchild, L. Y. Juravel and J. C. Woolley, J. Electron. Mater. 8, 25 (1979).

(36) H. Sakaki, L. L. Chang, R. Ludeke, Chin-An Chang, G. A. Sai-Halasz and L. Esaki, Appl. Phys. Lett. 31, 211 (1977).

(37) T. Waho, S. Ogawa and S. Maruyama, Jap. Appl. Phys. 16, 1875 (1977).